CEBAF Program Advisory Committee Nine Proposal Cover Sheet

This proposal must be received by close of business on Thursday, December 1, 1994 at:

CEBAF

User Liaison Office, Mail Stop 12 B

12000 Jefferson Avenue

Newport News, VA 23606

Proposal Title

Helicity Structure of Pion Photoproduction on Polarized Deuteron and the GDH Sum Rule for the Neutron.

Contact Person

Name: Zhujun Li

Institution: Christopher Newport University

Address: Dept. of Physics and Computer Science

Address:

City, State ZIP/Country: Newport News, VA 23606

Phone: (804) 249-7303 **FAX:** (804) 249-5800

E-Mail → Internet: LIZ@CEBAF.GOV

Experimental Hall: B **Days Requested for Approval:** 15

Hall B proposals only, list any experiments and days for concurrent running:

CEBAF Use Only

Receipt Date: 12/15/94 94-117

By: GP

Helicity Structure of Pion Photoproduction on Polarized Deuteron and the GDH Sum Rule for the Neutron

D. Doughty, L. Elouadrhiri, D. Heddle, and Zh. Li

Christopher Newport University, Newport News, VA

G.S. Blanpied, C. Djalali, B.M. Preedom, and C.S. Whisnant

University of South Carolina, Columbia, SC

B. Bertozzi, S. Gilad, A. Sarty, and Z. Zhao

MIT, Cambridge, MA

W. Brooks, V. Burkert, J.P. Chen, B.A. Mecking, and B. Niczyporuk

CEBAF, Newport News, VA

O.C. Kistner, A.M. Sandorfi, and C.E. Thorn

BNL, Upton, NY

S. Kuhn, C. Hyde-Wright, A. Klein, B.A. Raue, and L. Weinstein

Old Dominion University, Norfolk, VA

D.I. Sober, H. Crannell, and J.T. O'Brien

Catholic University of America, Washington, DC

S. Stepanyan

Yerevan Physics Institute, Yerevan, Armenia

L.Murphy

DAPNIA-SPhN, C.E.N. Saclay, 91191 Gif sur Yvette, France

R.A. Arndt, J. Ficenec, D. Jenkins, I. Strakovsky, and R. Workman

Virginia Polytechnic Institute and State University, Blacksburg, VA

R. Sealock

University of Virginia, Charlottesville, VA

S. Dytman, and D. Tedeschi

University of Pittsburgh, PA

P. Walch

Oregon State University, Corvallis, OR

K. Giovanetti

James Madison University, Harrisonburg, VA

M. Khandaker

Norfolk State University, Norfolk, VA

and the CLAS Collaboration

Spokespersons: J.P. Chen, S. Gilad, Zh. Li(contact) and C.S. Whisnant

Abstract

We propose to measure the cross section difference of the helicity-1/2 and helicity-3/2 contributions to single and two pion photo-production on the neutron at photon energies between 0.28 GeV and 2.2 GeV by using a novel polarized solid HD target, along with circularly polarized tagged photons and the CLAS detector. Since no double polarization measurement has previously been performed on the neutron, the measurement will be a major step towards a complete data set for a model-independent determination of the helicity amplitudes. The data will also enable a better study of resonances, especially those which are poorly determined.

We will also measure the total photon absorption cross section difference on the deuteron by simultaneously performing an inclusive hadron production measurement. All measurements will be performed nearly identically to and consecutively with the already approved proton measurements (E-91-015). Results on the neutron can be extracted from this experiment and E-91-015 by subtracting the proton cross section from that of deuteron. The results from this experiment, combined with low energy (pion threshold to 470 MeV) measurements from the LEGS facility at BNL, will allow a direct experimental test of the contributions to the GDH sum rule up to 2.2 GeV.

I. Introduction

1A. Single and two pion photoproduction

Pion photoproduction has provided important information on the resonance structure of the nucleon. In particular, photon decay coupling constants extracted from pion photoproduction data in the framework of partial wave analyses can be compared directly with quark models.

A precise and model independent determination of the partial wave amplitudes requires a vigorous experimental program of meson photoproduction. The experimental observables which can be expressed in terms of helicity amplitudes are the differential cross section $d\sigma/d\Omega$, the recoil polarization, the photon asymmetry, the target asymmetry and the double polarization observables. By choosing proper combinations of the polarization for the double polarization observables, one can get a complete set of measurements which determine the seven helicity amplitudes describing pseudoscalar meson production in a model-independent way.

With the exception of the recent Bonn[1]and BNL LEGS[2]measurements, all polarization measurements on the proton and the neutron were performed before 1981[3]. There are only scarce double polarization data on the proton. No data *at all* exist for the double polarization measurement (polarized beam and polarized target) on the neutron. Double polarization measurements on the neutron (deuteron target) will fill this vacuum, and add an essential part to the complete set of measurements needed to determine the helicity amplitudes. They, in turn, will provide us with important information on the structure of the nucleon resonances.

The polarization data on helicity cross section difference ($d\sigma = d\sigma_{1/2} - d\sigma_{3/2}$) or helicity asymmetry ($E = \frac{d\sigma_{1/2}-d\sigma_{3/2}}{d\sigma_{1/2}+d\sigma_{3/2}}$) will provide additional spin-dependent information on nucleon resonances. They are very sensitive to resonance structures and their parametrizations. As shown in Fig. 13, there are large differences between different phase shift analyses by VPI[4], Berends et. al.[5]and Moorhouse[6]at energies where resonances are not well determined (for example $P_{11}(1710)$, $D_{15}(1675)$ and $F_{15}(1680)$). Thus, the helicity asymmetry on single pion photoproduction will add a crucial constraint for the extraction of the partial wave amplitudes and the resonance parameters.

At the same time, helicity asymmetry on double pion photoproduction will provide a new tool to study those resonances with large branching ratios to two pion decay channels and relatively small ratios to single pion channels. Moreover, it is also a tool to search for missing resonances that decouple from single pion decay channel. A number of baryon resonances have been predicted by constituent quark models[7], but have not yet been seen.

These quark models suggest that these "missing" states have a very small decay ratio to πN states so that they escape the analysis of single pion production data. Yet, these resonance may have large enough photocoupling constants to be detected in the multipion final states.

1B. Gerasimov-Drell-Hearn sum rule

The Gerasimov-Drell-Hearn (GDH) sum rule[8]relates the total cross section of circularly polarized photons on longitudinally polarized nucleons to the anomalous magnetic moment of the nucleon:

$$\int_{thr}^{\infty}(\sigma_{1/2}-\sigma_{3/2})\frac{d\nu}{\nu}=-2\pi^2\alpha\frac{\kappa^2}{m^2}$$

where $\sigma_{1/2}$ and $\sigma_{3/2}$ are the total cross sections for hadron photoproduction on nucleons in the helicity 1/2 and 3/2 states, ν is the laboratory photon energy, κ is the anomalous magnetic moment, and m is the mass of the nucleon. The lower integration limit is the pion photoproduction threshold.

The GDH sum rule follows from the dispersion relation for forward Compton scattering along with the optical theorem and the low energy theorem. The forward Compton scattering amplitude may be written in terms of two scalar invariant functions of ν:

$$f(\nu)=f_1(\nu^2)\vec{e}'^{*}.\vec{e}+\nu f_2(\nu^2)i\vec{\sigma}.\vec{e}'^{*}\times\vec{e}$$

where $\vec{e}$ and $\vec{e}'$ are the transverse polarization vectors of the incident and forward-scattered photon, respectively. Causality implies analyticity of f_2 which allows us to write the dispersion relation for the forward amplitude without subtraction:

$$\mathrm{Re}f_2(\nu^2)=\frac{2}{\pi}\mathrm{P}\int_0^{\infty}d\nu'\frac{\mathrm{Im}f_2(\nu'^2)\nu'}{\nu'^2-\nu^2}.$$

Unitarity can be expressed in the optical theorem:

$$\mathrm{Im}f_2(\nu^2)=\frac{1}{8\pi}(\sigma_{1/2}-\sigma_{3/2})$$

The low energy theorem[9], which comes from gauge invariance and relativity, tells us that

$$f_2(0)=-\frac{\alpha\kappa^2}{2m^2}.$$

Combining the above equations, the GDH sum rule follows immediately. The no-subtraction assumption ($\mathrm{Re}f_2(\infty)=0$) and the assumption that the cross section difference falling off

with energy faster than $1/\nu$ could be open to 'reasonable' questions. The generality of the input assumptions suggests very strongly that the sum rule should be verified, which has become possible now with the technical development in polarized beams, targets and large acceptance detector at CEBAF.

Because of the $1/\nu$ weighting in the integrals, single pion photoproduction is expected to have a sizeable contribution to the GDH sum rule (dominant at low energy). Using the results of multipole analyses of the existing (mostly unpolarized) data, Karliner[10]and more recently Workman and Arndt[11], Burkert and Li[12], and Sandorfi et al.[13]have computed the single pion contribution to the GDH sum rule for the proton and the neutron, with some estimates of the inelastic contribution included. These values are compared to the GDH prediction in Table 1. Also listed are the values calculated based on an extended current algebra (ECA) model[14], in which the GDH rum rule is modified by adding another term to the assumption of the 'no-subtraction' dispersion relation. Sandorfi et al.'s calculation used the most recent VPI partial-wave analysis result that have included the recent polarization data from Bonn and BNL (ref. 1 and 2). The major difference between this calculation and the one of Workman and Arndt which is based on an older VPI partial-wave analysis is in the vector scalar interference term. The fact that this term depends so critically on the polarization data further strengthens our motivation for a double polarization measurement.

It is particularly interesting to notice that the proton-neutron sum rule (which is equivalent to the isoscalar-isovector interference sum rule) has a different sign from the partial wave analysis results, and is far from saturation by the existing calculation up to 1.8 GeV. It will be of great interest to experimentally test the GDH rum rule on the proton, and the neutron, and especially their difference.

Table 1. Various Calculations for the GDH Sum Rule

	DHG(p)	DHG(n)	DHG(p-n)
DHG sum rule	-204.5 μb	-232.8μb	28.3μb
Analysis by Karliner	-261 μb	-183 μb	-78 μb
Analysis by Workman and Arndt	-257 μb	-189 μb	-68 μb
Analysis by Burkert and Li	-203 μb	-125 μb	-78μb
Analysis by Sandorfi et. al.	-289 μb	-160 μb	-130μb
Extended Current Algebra	-294 μb	-185μb	-109μb

The recent interest in the GDH sum rule is also due to Anselmino, Burkert, Ioffe and others[15]. These authors try to connect the GDH sum rule with g_1, the spin structure function of the nucleon, in an attempt to understand the nucleon 'spin crisis' raised by the results of the EMC experiment[16]and early SLAC experiments[17]. Recent results on the spin structure functions of the proton from SLAC E143[18]confirm the EMC result and the result on deuteron from the SMC[19]is also consistent with the EMC result, while the result on neutron from SLAC E142[20]experiment apparently 'disagrees' with the EMC/SMC results, if the Bjorken sum rule[21]is assumed valid. The E142 result shows almost no 'spin crisis'. Since the three experiments were performed at different Q^2, the Q^2 dependence of the spin structure function became an important issue. The GDH sum rule gives the prediction at $Q^2 = 0$ (real photon) point which can be related to the spin structure functions in electron (or muon) scattering by

$$\sigma_{1/2} - \sigma_{3/2} = \frac{8\pi^2\alpha}{\nu - Q^2/2m}(m\nu G_1(Q^2,\nu) - Q^2 G_2(Q^2,\nu)).$$

For deep-inelastic scattering and real photo-absorption, the second term vanishes, and $\sigma_{1/2} - \sigma_{3/2}$ can be expressed simply in terms of G_1. Anselmino et al. defined the following quantity:

$$I(Q^2) = m^3 \int_{Q^2/2m}^{\infty} \frac{d\nu}{\nu} G_1(Q^2,\nu) = \frac{2m^2}{Q^2}\int_0^1 dx g_1(Q^2,x)$$

which, at $Q^2 = 0$, is given by the GDH sum rule:

$$I(0) = \frac{m^2}{8\pi^2\alpha}\int_{thr}^{\infty}(\sigma_{1/2} - \sigma_{3/2})\frac{d\nu}{\nu} = -\frac{\kappa^2}{4}.$$

The deep inelastic results from EMC/SMC/E142/E143 indicate that $I(Q^2)$ has to change dramatically between $Q^2 = 0$ and the deep inelastic region. This is the subject of three other CEBAF experiments (E-91-023, E-93-009 and E-94-010)[22]which will measure the polarized structure functions for both the proton and the neutron covering the Q^2 range from 0.15 to 2 $(GeV/c)^2$.

One experiment on the proton GDH sum rule (E-91-015)[23]at the real photon point has been approved at CEBAF with no specific target. We are proposing to use the new HD target in both the E-91-015 and this experiment. With the HD target, we propose to make deuteron measurements consecutively and identically with the proton measurements. This will help in extracting neutron data with reduced systematic uncertainty. By using the new HD target, we will not only significantly reduce background, compared to the previously used NH_3/ND_3 (or $C_8H_{10}O/C_8D_{10}O$) targets, but also save beam time due

to the much smaller dilution factor. The target is currently under development by the LEGS-spin collaboration[24]. It will be first used in a LEGS experiment in early 1996.

The photon energy covered by the experiment will be from 0.28 GeV up to 2.2 GeV. A similar experiment[24] at BNL LEGS will cover the energy from single pion threshold to 0.47 GeV. Most of the resonance contributions, which are expected to be the main contribution to the sum rule, are covered in the energy range below 2 GeV.

In order to test the convergence of the GDH sum rule it is necessary to extend the measurement to higher photon energies by utilizing the 4 GeV or even 6 GeV electron beam at CEBAF. We intend to carry out a detailed study at these energies.

II. Experimental Setup

2A. Circularly polarized photon beam

A circularly polarized photon beam can be produced by bremsstrahlung of longitudinally polarized electrons. The circular polarization is given approximately by [25]

$$P_{circ} = P_{el}(4x - x^2)/(4 - 4x + 3x^2)$$

where $x = \nu/E_0$ (E_0 is the electron energy, and ν the photon energy), and P_{el} is the longitudinal polarization of the electrons. A more precise calculation requires angular integration over the collimation aperture. Some results are plotted in Figure 1.

The development of polarized electron sources has advanced tremendously over the last few years. In a recent experiment at SLAC (E143), electron polarization of more than 80% with an average beam current of more than 80 nA was achieved routinely using strained GaAs cathodes. We assume that 80% electron polarization will be available at CEBAF by the time the proposed experiment will run. The photon circular polarization will be close to 100% of the electron polarization at the high energy endpoint and will slowly decrease to $> 50\%$ of the electron polarization for $\nu/E_0 = 0.5$. We plan to use only the upper part of the bremsstrahlung spectrum. Table 2 shows the polarization for the proposed kinematics.

Table 2. Photon Beam Polarization

E_0(GeV)	ν_{min}(GeV)	ν_{max}(GeV)	P_{min}	P_{max}	P(Ave)
0.8	0.28	0.76	34%	80%	$> 50\%$
1.6	0.70	1.52	44%	80%	$> 60\%$
2.4	1.40	2.28	59%	80%	$> 70\%$

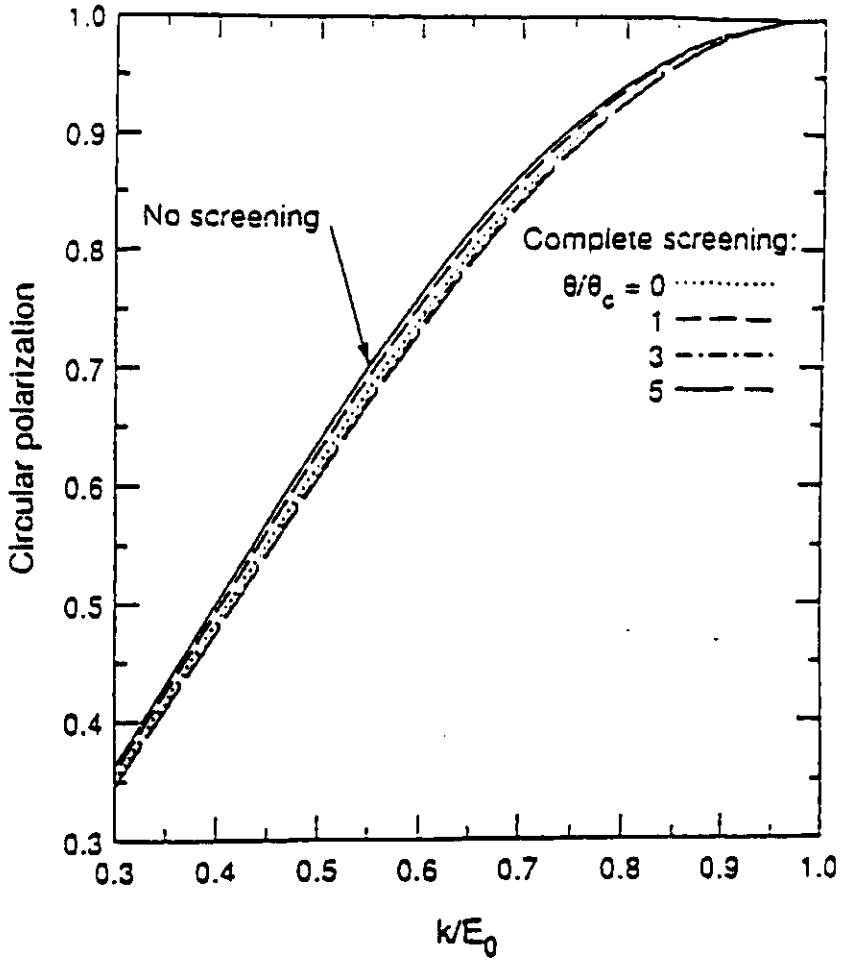

Figure 1. Circular polarization of bremsstrahlung from a 100% *longitudinally polarized electron. The different 'complete screening' curves (calculated in Ref. 25) show the dependence of photon emission angle in units of* $\theta_c = m_e/E_0$.

To cover the range from 280 MeV to 2.2 GeV, three electron energies settings are needed: 0.8, 1.6, 2.4 GeV. The Hall B tagging system will be used to produce tagged photons at a rate of $10^7\gamma$/second. The photons will be collimated to a diameter of about 2 cm, consistent with the size of the target. Because of the collimation, the rate of tagged photons on target will be less than the total tagging rate.

The Hall B Möller and/or Compton polarimeter will be used to measure the beam polarization. An uncertainty of less than 4% is expected.

2B. Polarized solid HD target

SPHICE, a Strongly Polarized Hydrogen and Deuterium ICE target, represents a new technology utilizing molecular HD in the solid phase. This target offers several advantages

for polarized nucleon measurements compared to those that are currently in common usage. Because the only polarized species in this target are hydrogen and deuterium and there is only 5% unpolarized material (by weight), much smaller backgrounds are expected for many reactions, making it possible to measure not only asymmetries but absolute cross sections. At present there are no absolute cross section data taken with polarized hydrogen or deuterium targets with real photons. SPHICE will provide the first opportunity. The dilution factors are quite advantageous: one half of the protons are free and polarizable and all the deuterons are polarizable. Since the polarizing facility is not in-beam, the in-beam dewar is simplified, making large solid angle available. The expected proton and deuteron polarizations of about 80% and 50%, respectively, are comparable to that achieved with conventional materials. Using rf techniques, the H and D spins can be oriented independently allowing all beam-spin/target-spin/holding-field combinations to be explored. This has a major positive impact on systematic errors.

Such a target is being developed for nucleon spin structure measurements at LEGS by the LEGS-Spin collaboration[24]. A feasibility study begun in 1993 has been completed and the production phase has begun. Some of the historical developments are recounted in a paper presented at the 7th International Workshop on Polarized Target Materials and Techniques held in Bad Honnef, Germany, in June 1994[26]. The paper also includes data from very recent investigations of this target, in particular the results of experiments in which very long relaxation times (depolarization times) were obtained, ranging from the order of weeks to over a year. Such relaxation times are the key to efficient use of these targets, especially with weakly ionizing beams, since target utilization time in an experiment can now be well-matched to the target polarization-production time.

Arnold Honig of Syracuse University has been studying hydrogens in the solid state since the 1960's and has produced small volume polarized HD ice targets for inertial confinement fusion experiments[27][28][29]. These targets are polarized at low temperature and high field in a dilution refrigerator. The spin-lattice coupling which permits polarization (and depolarization) of these targets is effected by small ($\approx 10^{-4}$) concentrations of ortho-H_2 (molecular rotational angular momentum, J = 1). Since this decays to J=0 para-H_2 with a time constant of 6.25 days, the relaxation time is a function of the time the target is held in the polarizing conditions. This is the so-called "relaxation switch". Once the polarization relaxation time has increased sufficiently, the targets are extracted using a specially designed transfer dewar. These frozen spin targets can then be stored or transported by inserting them in a storage dewar (4K/8T) and can be used at modest fields and temperatures that are compatible with experimental conditions. In the fall of 1992 a collaboration including South Carolina, Syracuse, BNL IN2P3 (Orsay, France), and INFN

(Frascati, Italy) was formed to support a feasibility study for such a target. The feasibility study addressed two issues: the extrapolation to very long spin relaxation times and heat removal from the large volumes required for practical targets. At 1.5K, relaxation times ranging from about 1 week at a 1 Tesla holding field to nearly one year at 8T were observed. The removal of heat generated by the J=1 to J=0 conversion during the polarization phase requires the threading of thin ($\leq 25\mu m$) aluminum wire through the target. This produces a target that is 5% (unpolarized) aluminum by weight (the number of protons in aluminum nuclei is 7% of the number of hydrogen nuclei.). Using the results of this study, holding field and temperature criteria were established for in-beam operation as well as the large dilution refrigerator. The feasibility study has shown that the technology developed by A. Honig can indeed be extended to useful nuclear physics targets and the results were presented to a BNL technical review panel in June 1994. As a result of the review, BNL has now ordered the large dilution refrigerator and high field polarizing magnet. Orsay is constructing the transfer and in-beam dewars for the LEGS experiments. South Carolina is responsible for the superconducting Helmholtz coil which will produce a 1 Tesla holding field in-beam.

Target Production and Usage

The target polarization procedure is described in detail in the appendix and is summarized here. The polarization cycle is begun by placing an HD target suitably doped with o-H_2 in a high magnetic field (17 T) at low temperature (15 mK). Because of the coupling between the spins of the hydrogen in HD and the lattice effected by the o-H_2 impurity, the proton spins can align with the field and the hydrogen reaches about 80% polarization. The smaller deuteron magnetic moment and its much weaker coupling with the lattice requires another technique for producing high deuteron polarization. The weak dipolar coupling between the H and D spins in neighboring nuclei permits the use of the adiabatic fast passage rf technique for transferring some of the hydrogen polarization to the deuterium[30]. The hydrogen is then repolarized in the high field. Although the spin-lattice relaxation time is continually increasing, a second transfer is possible, bringing the deuterium polarization up to 50%. Once both species are polarized, the target is held at the high field/low temperature conditions until the concentration of o-H_2 has decreased sufficiently to produce usable spin-lattice relaxation times. This entire process takes about 45 days and produces targets with useful lifetimes of at least a week. If only hydrogen polarization is desired, the adiabatic fast passage transfers are omitted. If only deuterium polarization is required, the hydrogen polarization can be quenched using rf. Thus, a target in which either hydrogen or deuterium or both are polarized can be produced.

The technological step that makes such a target practical for a scattering experiment

is the transfer dewar[27]. This is a LHe/LN_2 dewar that one can insert into the dilution refrigerator, connect to the polarized target, remove it and place it in a low field, warm environment for experimental use. This permits the use of a much simpler in-beam dewar than is currently used for other polarized targets.

This extraction dewar has been developed as a part of the laser fusion work carried out by Honig. A schematic is shown in Figure 2. The dimensions for this device are matched to the dilution refrigerator being used and designs for the SPHICE target are in progress at Orsay. The refrigerator required for production of the proposed nuclear physics target is necessarily large, making the extraction dewar about 1.5-2 meters long. The liquid helium dewar, terminating in the 4K cold finger (Figure 2, upper left), can be rotated and translated inside the surrounding liquid nitrogen dewar (upper right). Thus, it is possible to insert this device in the top-loading refrigerator and screw it into a left/right threaded coupling on the target cell. The target is retracted into the shroud and a leaf shutter closes over the end. The target is now in a 4 K environment suitable for removal from the refrigerator. The holding field is provided by a high critical temperature superconducting coil (not shown).

Additional dewar/magnet systems will also be constructed to provide a temporary storage and transportation of the targets. These dewars will be a ^{4}He cryostat with an 8 Tesla magnet. At 8T and 1K the relaxation time is increased to about 1 year. Thus, if there are facility problems preventing the use of the target, it can be efficiently stored without significant loss in polarization. With polarization production times of about 40-50 days, target aging experiments (see the discussion of the feasibility study in the appendix) have demonstrated that we can have useful target lifetimes with the target held at temperatures between 0.45K and 1.5K. At 1 Tesla, proton polarizations can be maintained for at least a week. The increase in the relaxation times at the lower temperatures means that the average proton polarization can be as high as 88% of the initial value and the average deuteron polarization even higher. Efficient target usage requires that the production time be comparable to the resulting relaxation times. This can be realized by polarizing four targets simultaneously. By loading four targets, in tandem, into the dilution refrigerator, each one can be sequentially polarized with the rf technique. This allows simultaneous aging of four targets with little additional time added to the polarizing cycle. This is shown schematically for two targets in Figure 3. Thus, after $\approx$ 45 days, four targets are produced, each with at least 1 week useful life. Transferring these from the dilution refrigerator to a turreted storage dewar holding the targets at 1.5K and 8 Tesla provides storage times of nearly 1 year. While these four target are used in-beam, the next four are in preparation. In this way, targets are continuously available.

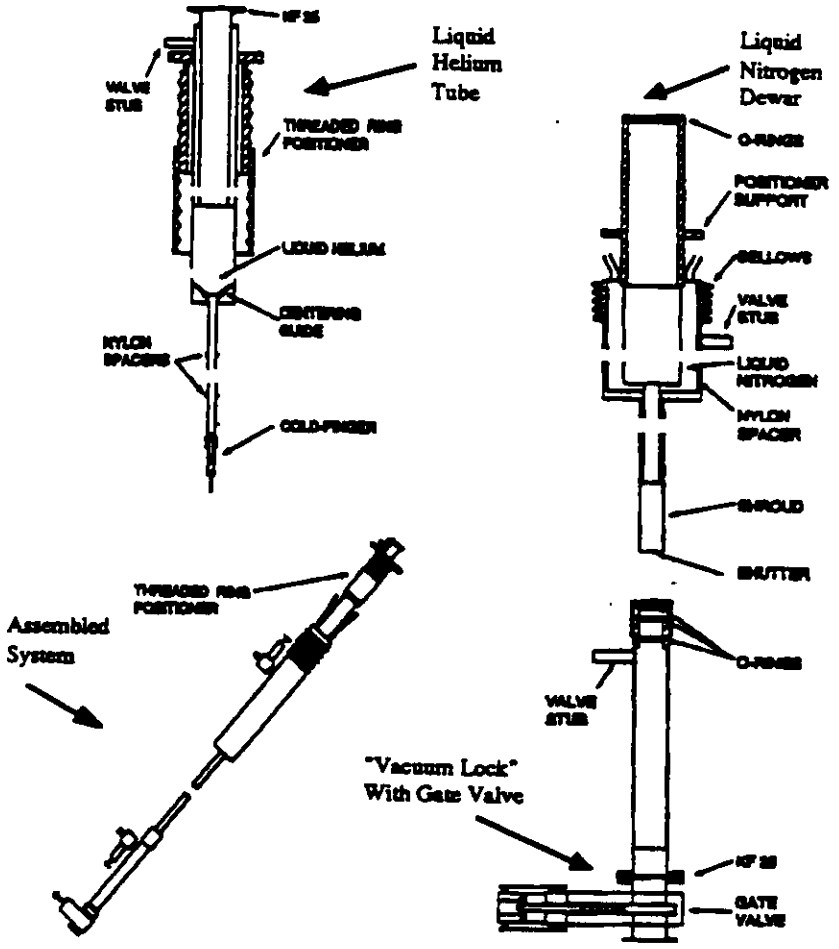

Figure 2. Schematic of an existing transfer dewar. The scales are not indicated on drawing since the one to be constructed for the SPHICE target will be larger. These drawings represent one successfully used for transferring small polarized HD targets from a dilution refrigerator at Syracuse University for transport to the OMEGA laser fusion facility, 50 miles away in Rochester, NY.

The long storage times and the ability to transfer the target from one dewar to another permit the production and usage facilities to be quite far apart. Honig has demonstrated this by producing small targets at Syracuse and transporting them to Rochester, NY for laser fusion experiments at the Omega facility. The SPHICE target will be produced in Syracuse and shipped to LEGS for the initial experiments. Once production techniques are well developed, the production facility will be moved to LEGS. This move is expected to take place in about two years. For the experiments at CEBAF the targets will be polarized

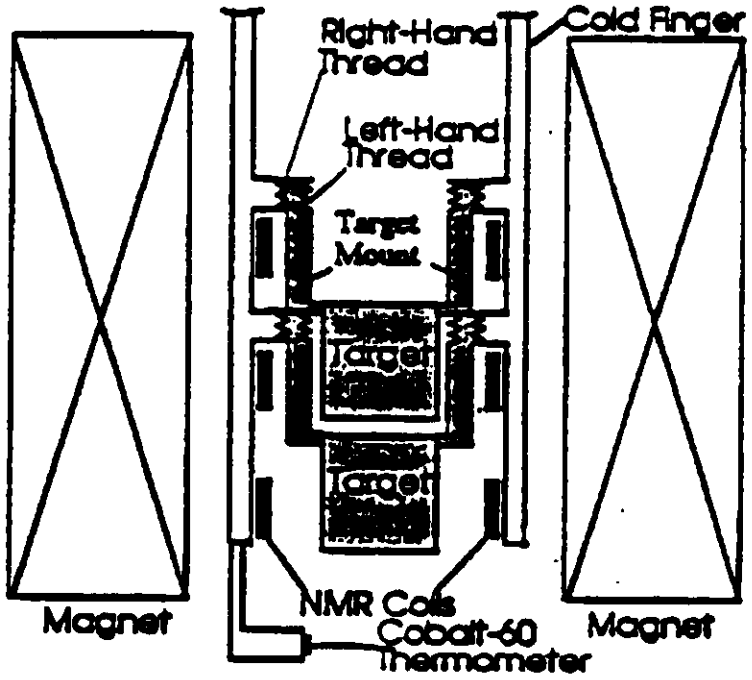

Figure 3. Schematic drawing showing two of the four targets loaded for polarization.

at BNL and shipped to Newport News.

The CLAS Target

A detailed design of the in-beam dewar design for the LEGS experiment is in progress at Orsay. A preliminary sketch of an in-beam dewar suitable for CLAS is shown in Figure 4. The holding field at LEGS will be supplied by a superconducting Helmholtz coil with a diameter of 32 cm. This permits the field to also be used to discriminate π^+ and π^- by observing the bend direction in the field. For the proposed experiments at CLAS, a superconducting solenoid is more appropriate. Such a coil has been built at Bonn for the longitudinally polarized target being constructed for the spin structure measurements at Bonn and Mainz. This coil will add 500μm of material to the wall thickness (300μm of copper carrier, 150 μm superconducting wire and 50 μm resin to fix the wire on the carrier). This configuration will also be used at LEGS while the Helmholtz coil and associated wire chambers are being prepared.

Once a target has been successfully used in experiments at LEGS, final designs for the in-beam dewar and storage cryostats required for this experiment will begin.

The anticipated target size is about 2.5 cm in diameter and 7 cm long. This gives a

target with $\rho t = 1.1$ g/cm^2 HD. The diameter is limited by the bore of the top-loading dilution refrigerator and the volume is set by the cooling capacity of the refrigerator.

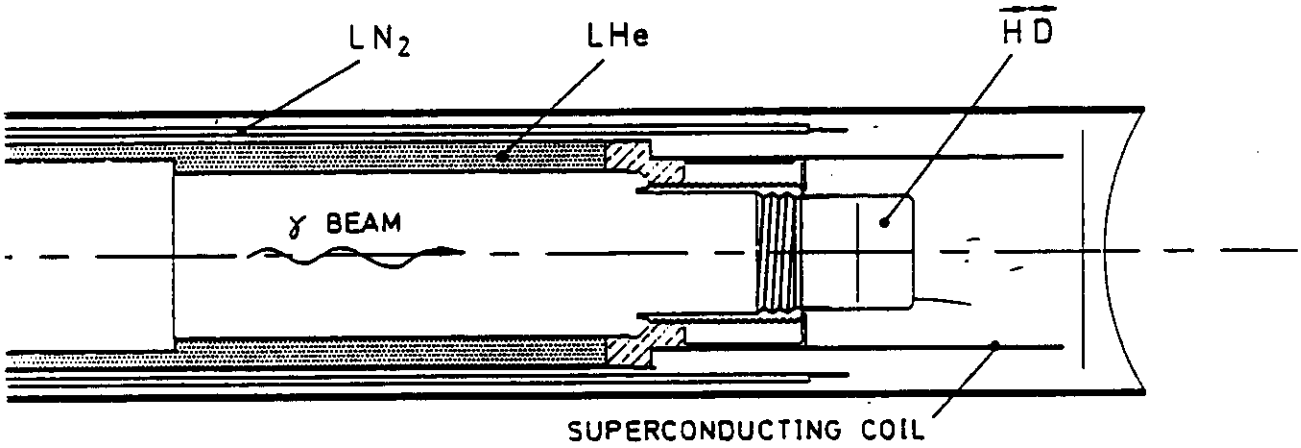

Figure 4. A preliminary sketch of the in-beam dewar.

2C. Detector

To measure the pion photoproduction and total hadronic photoabsorption cross sections, a large acceptance detector is needed to obtain the maximum angular coverage. CLAS is well suited for this purpose. The angular range for charged particle detection is from $\sim 7°$ to $\sim 135°$ [31]. The magnetic field of the CLAS toroid will be set to bend the π^- and other negatively charged particles into the detector from smaller angles (See fig. 5 for a Monte Carlo SDA simulated event in the CLAS detector). The forward angle electromagnetic calorimeter, which has good neutral particle detection efficiency, covers $\sim 7°$ to $\sim 45°$ and the large angle calorimeter covers one sector (out of six) of 45° to 90°. The detection efficiency for photons from π^0 decay is nearly 100%. For neutrons the detection efficiency varies with the neutron momentum, it can reach 60% (see Fig.6 for a GEANT simulation). The neutron detection efficiency will be calibrated simultaneously during the experiment to a precision of better than 3% using the process $\gamma p \to \pi^+ n$

III. Proposed measurements

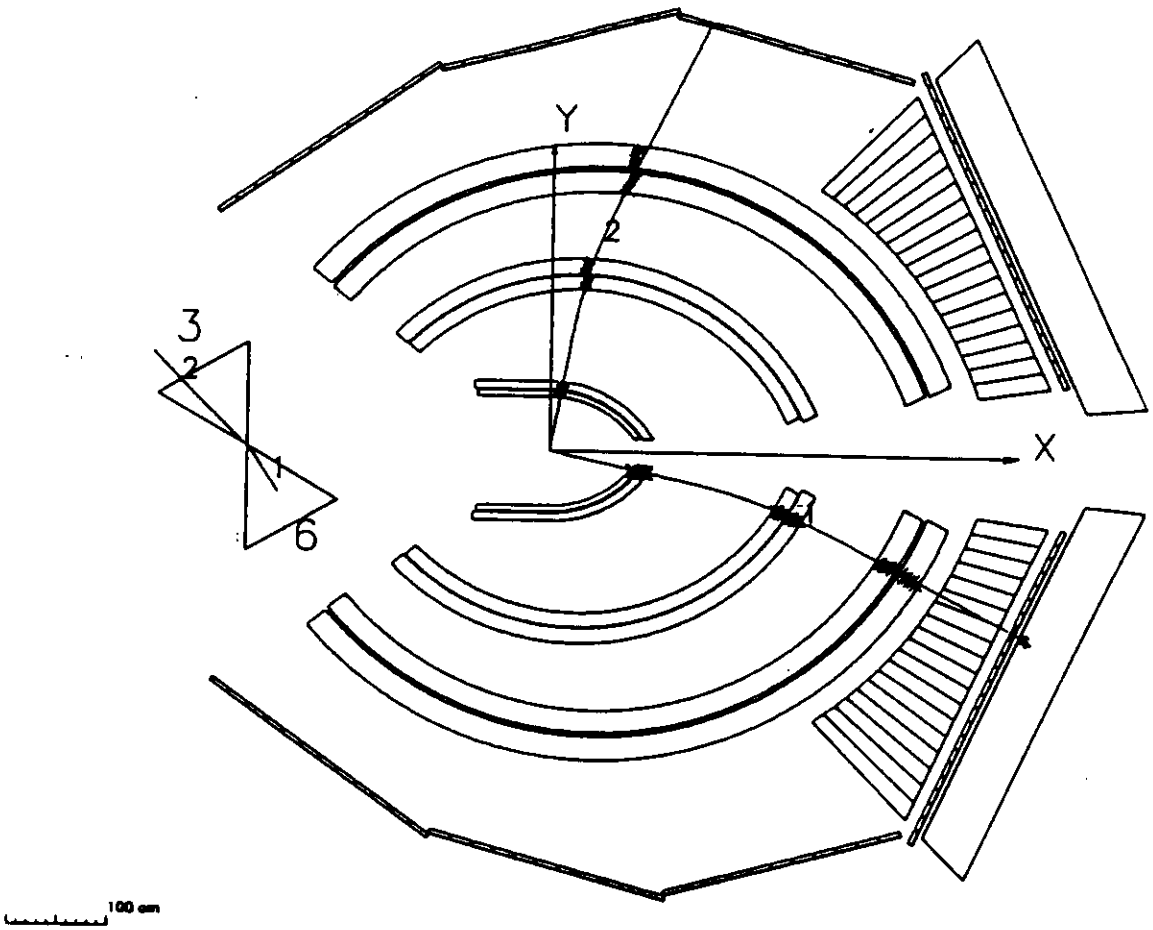

Figure 5. A Monte Carlo SDA simulated event in the CLAS detector for $\gamma n \rightarrow \pi^- p$, track 1 is the π^- at 10°, track 2 is the proton.

The target proton and deuteron polarizations can vary independently due to their different rf energy splittings. For the deuteron measurements we will have maximum deuteron polarization and zero proton polarization and vice versa for the proton measurements. When two measurements (A and B) are performed with p(d) polarizations of $P_p^A(P_d^A = 0)$ and $P_d^B(P_p^B = 0)$, then the helicity cross section difference ($d\sigma = d\sigma^{1/2} - d\sigma^{3/2}$) for proton and deuteron can be obtained:

$$\Delta d\sigma^p = \frac{\Delta d\sigma_A}{P_p^A}$$

and

$$\Delta d\sigma^d = \frac{\Delta d\sigma_B}{P_d^B}.$$

During the entire experiment, the polarization direction will be reversed frequently for the photon beam and also (much) less frequently for the target to reduce systematic errors. The two measurements (A and B) will be done consecutively under the same conditions except that the magnetic field in the deuteron measurement will be reversed.

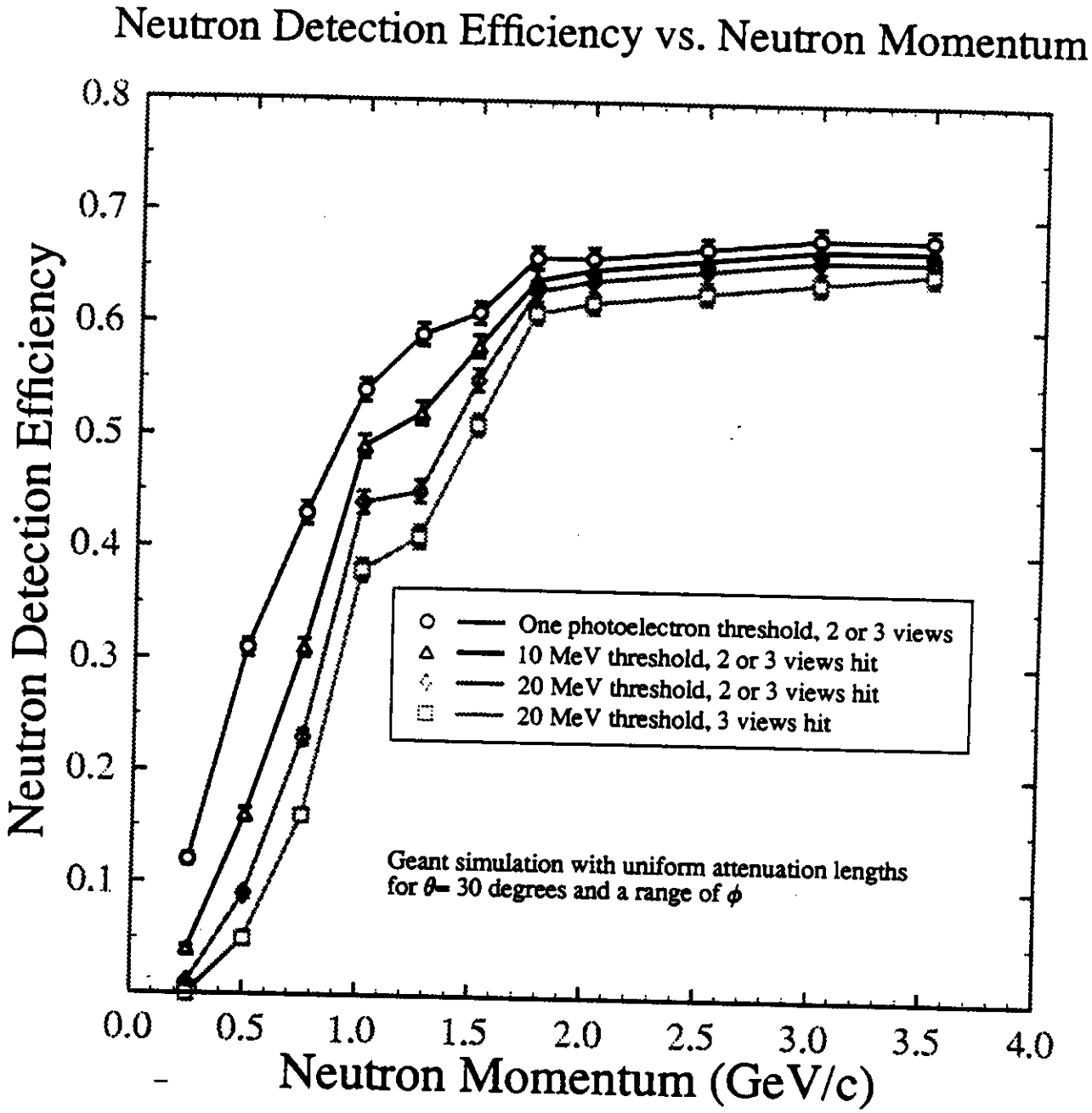

Figure 6. GEANT simulation of neutron detection efficiency in the electromagnetic calorimeter[32]

3A. Exclusive single pion production

In single pion production on the neutron case, there are only two channels:

$$\vec{\gamma} + \vec{d} \rightarrow \pi^- + p + p_s \quad (1)$$

$$\vec{\gamma} + \vec{d} \rightarrow \pi^0 + n + p_s \quad (2)$$

where the subscript 's' indicates a spectator nucleon. The pion will be detected in coincidence with the outgoing nucleon. In cases where only pions can be detected, missing mass reconstruction will be used to identify the process.

The partial-wave analyses based on the existing single pion photoproduction data can be used as a guidance for studying the detector response. Here we have used the VPI partial-wave analysis results for this purpose. Fig.7 shows the VPI calculation of the total cross section for both π^- and π^0 production on the neutron and the sum of the two processes, compared with the total photo absorption cross section measurements[32], and the VPI differential cross section calculation at $\theta_{cm} = 60°$ compared with the world data. Fig.8 shows the total helicity cross section ($\sigma_{1/2}$ and $\sigma_{3/2}$) for π^- and π^0 production on the neutron. Fig.9 shows the differential helicity cross section at photon energies 0.4, 1.0 and 1.8 GeV. These figures demonstrate that the cross sections in the interesting energy region are sizable.

An event generator based on the VPI results has been developed for this proposal, which provides realistic angular and energy distributions for single pion photoproduction. Detailed simulation of the CLAS detector response has been performed using SDA for charged particle and FASTMC for neutral particle detection.

Fig.10 shows the acceptance and missing mass reconstruction of the proton at photon energies of 0.7 and 1.0 GeV for the $\pi^- p$ channel. We see a large acceptance as well as very good angular coverage. Missing mass resolution will be sufficient to separate single pion events from muti-pion events (also refer to Fig.12).

Fig.11 shows the acceptance and missing mass reconstruction of the neutron at photon energies 0.7 and 1.5 GeV for the $\pi^0 n$ channel. It shows that the acceptance for coincidence measurements is small and has very limited angular coverage. Using missing mass reconstruction, we will be able to measure the forward angular range where pions are detected. Above threshold, the $\gamma n \rightarrow \pi^0 n$ channel can be calculated from the other three channels using isospin symmetry.

Our simulation study shows that we will be able to measure the helicity cross section difference or helicity asymmetry with high statistical accuracy.

3B. Exclusive two-pion production

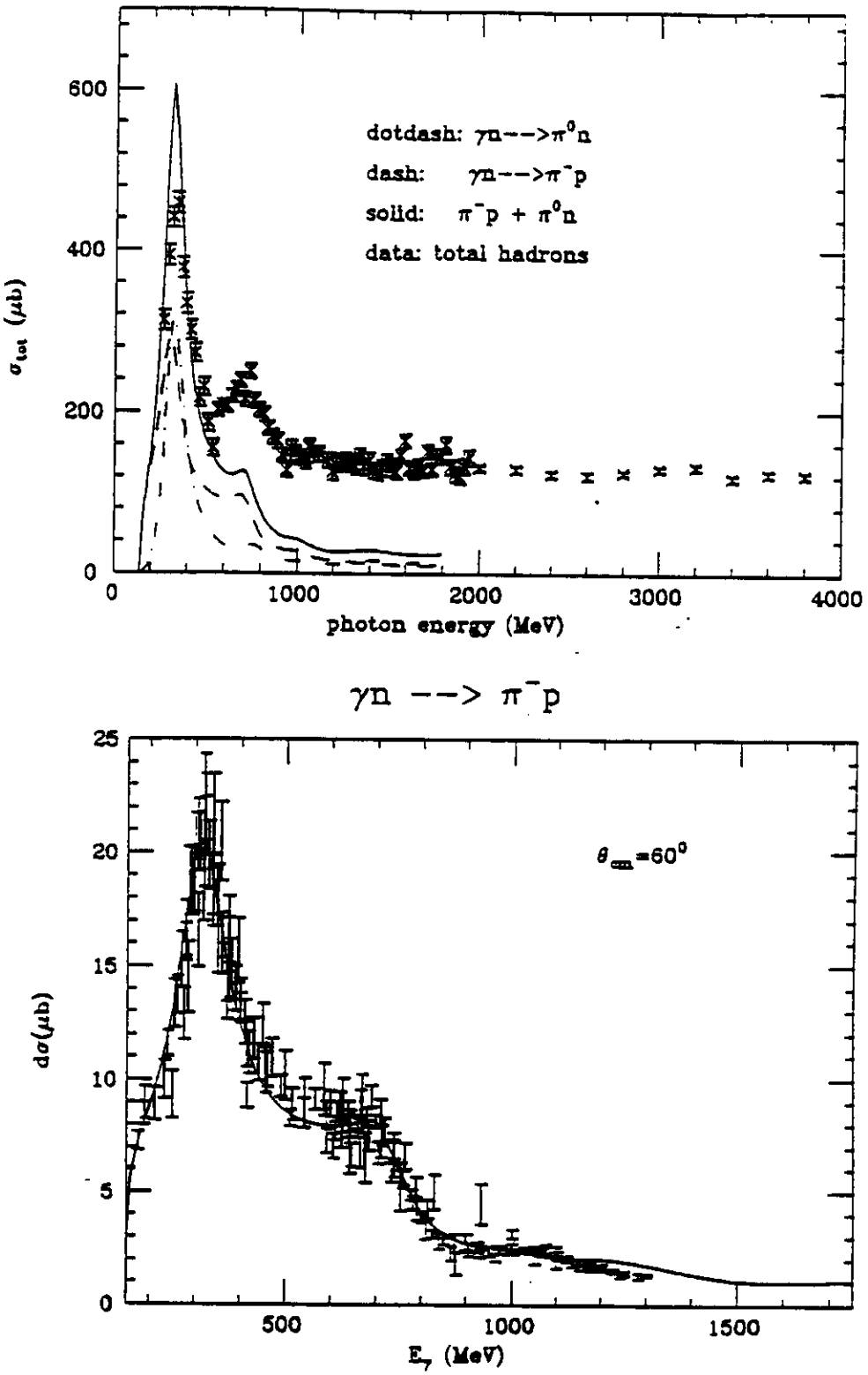

Figure. 7. Total single pion photoproduction cross section calculated from the VPI partial-wave analysis, along with the total photo-neutron cross sections ($\gamma n \rightarrow hadrons$[33]) (top) and the differential single pion photoproduction cross section calculated from the same analysis along with the world data at $\theta = 60^0$ (bottom).

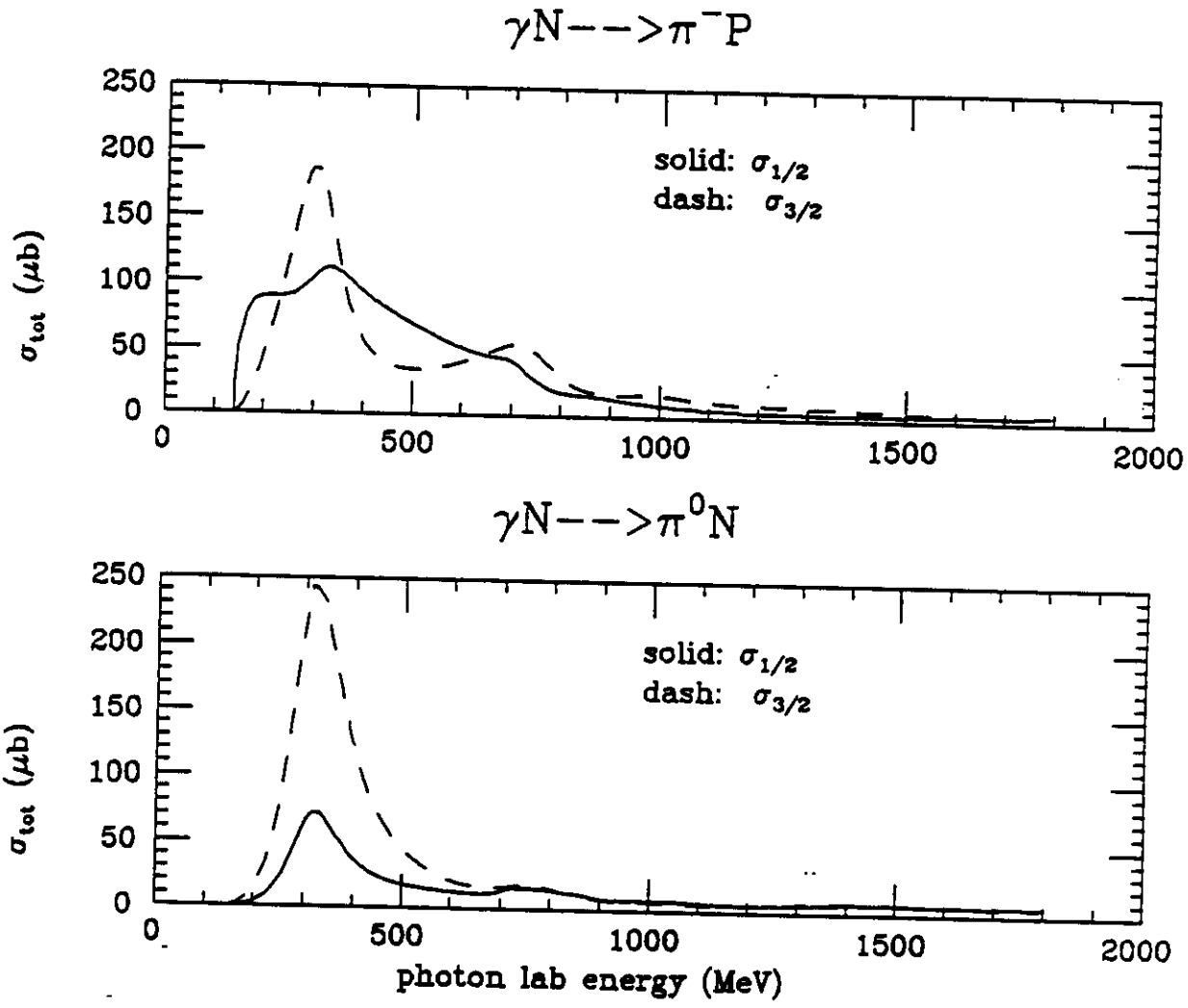

Figure 8. Total single pion photoproduction cross sections for helicity 1/2 and 3/2, calculated from the VPI partial-wave analysis.

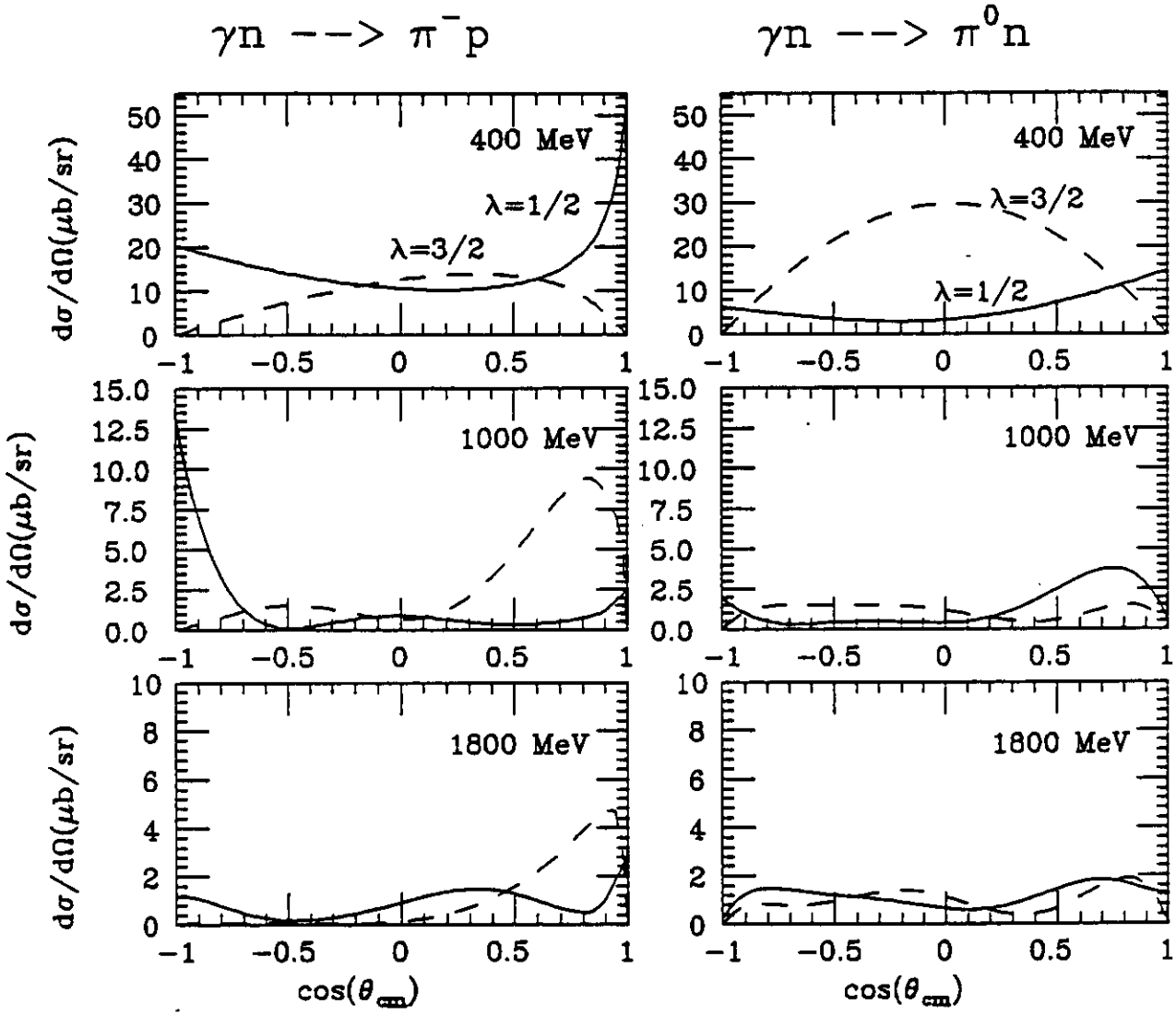

Figure 9. Single pion photoproduction differential cross sections calculated from the VPI partial-wave analysis. Solid curves are for helicity 1/2, and dashed curves for helicity 3/2.

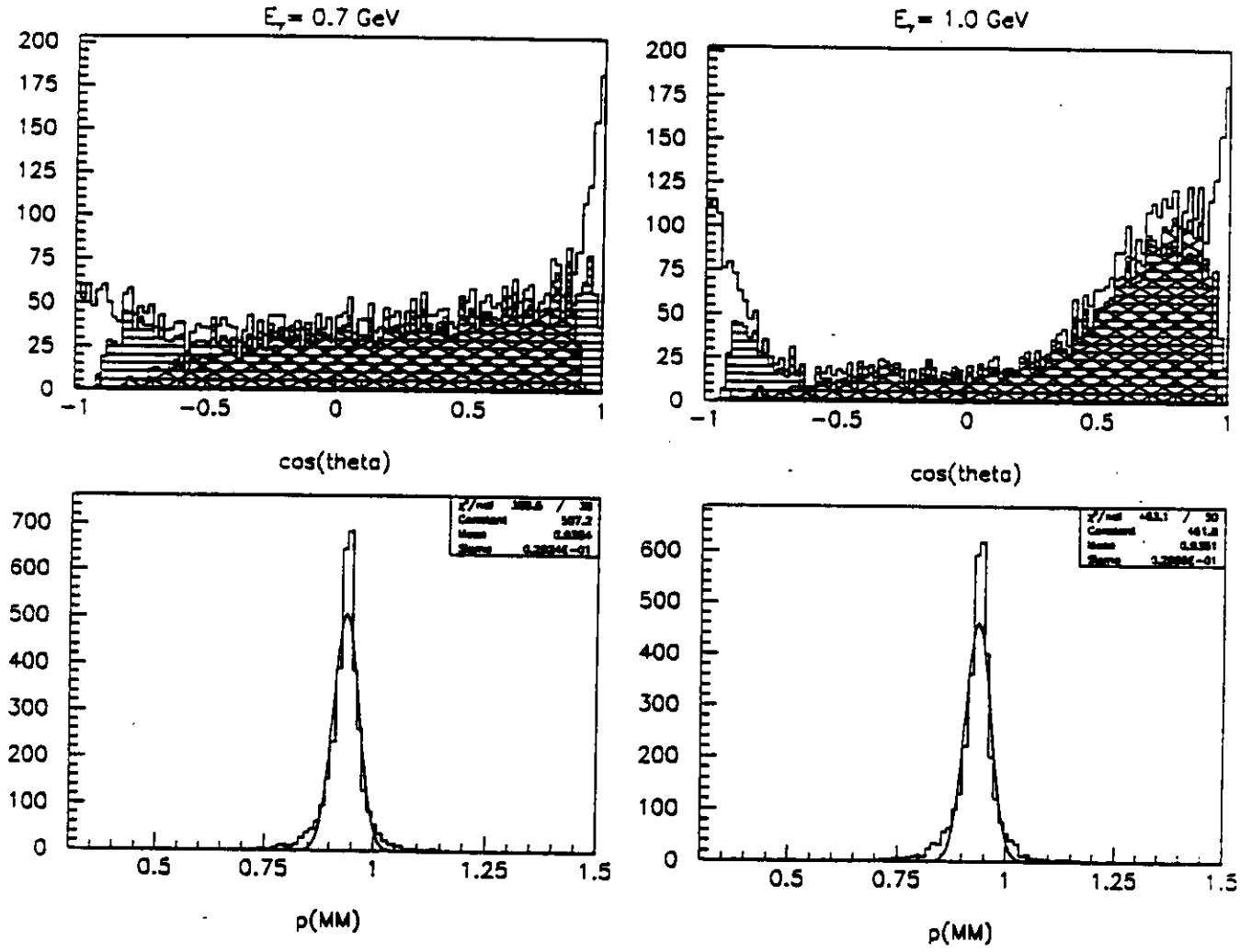

Figure 10. SDA simulation results for $\gamma d \rightarrow \pi^- pp_s$ at $E_\gamma = 0.7$ and 1.0 GeV: acceptance for π^- and p, respectively, versus the pion center of mass angle cosθ (top). Missing mass resolution for the proton when only the π^- is detected (bottom).

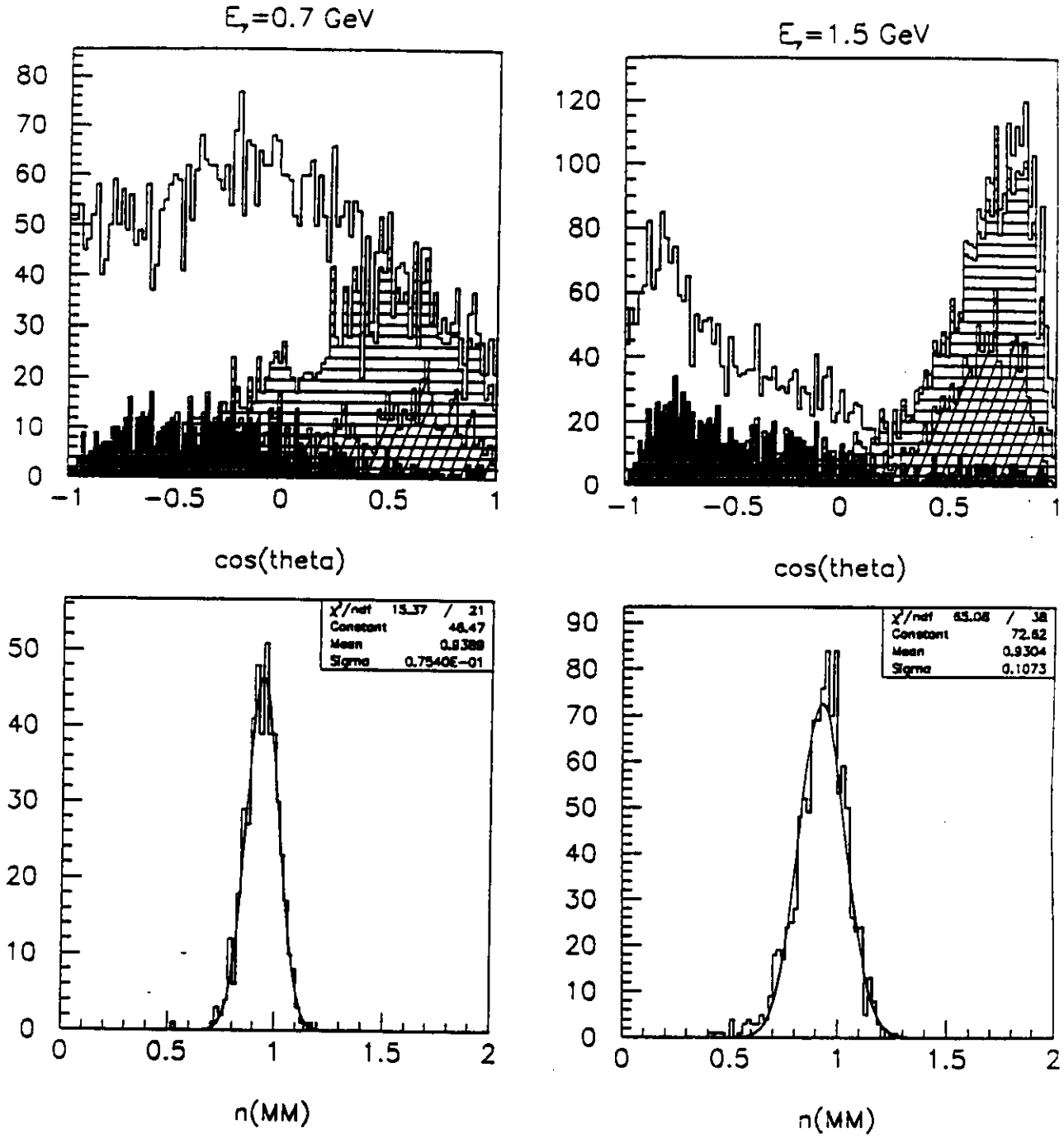

Figure 11. FASTMC simulation results for $\gamma d \rightarrow \pi^0 n p_s$ at $E_\gamma = 0.7$ and 1.0 GeV: acceptance for one γ, π^0 and n, respectively, versus the pion center of mass angle, $cos\theta$, (top). Missing mass resolution for neutrons when only the π^0 is detected (bottom).

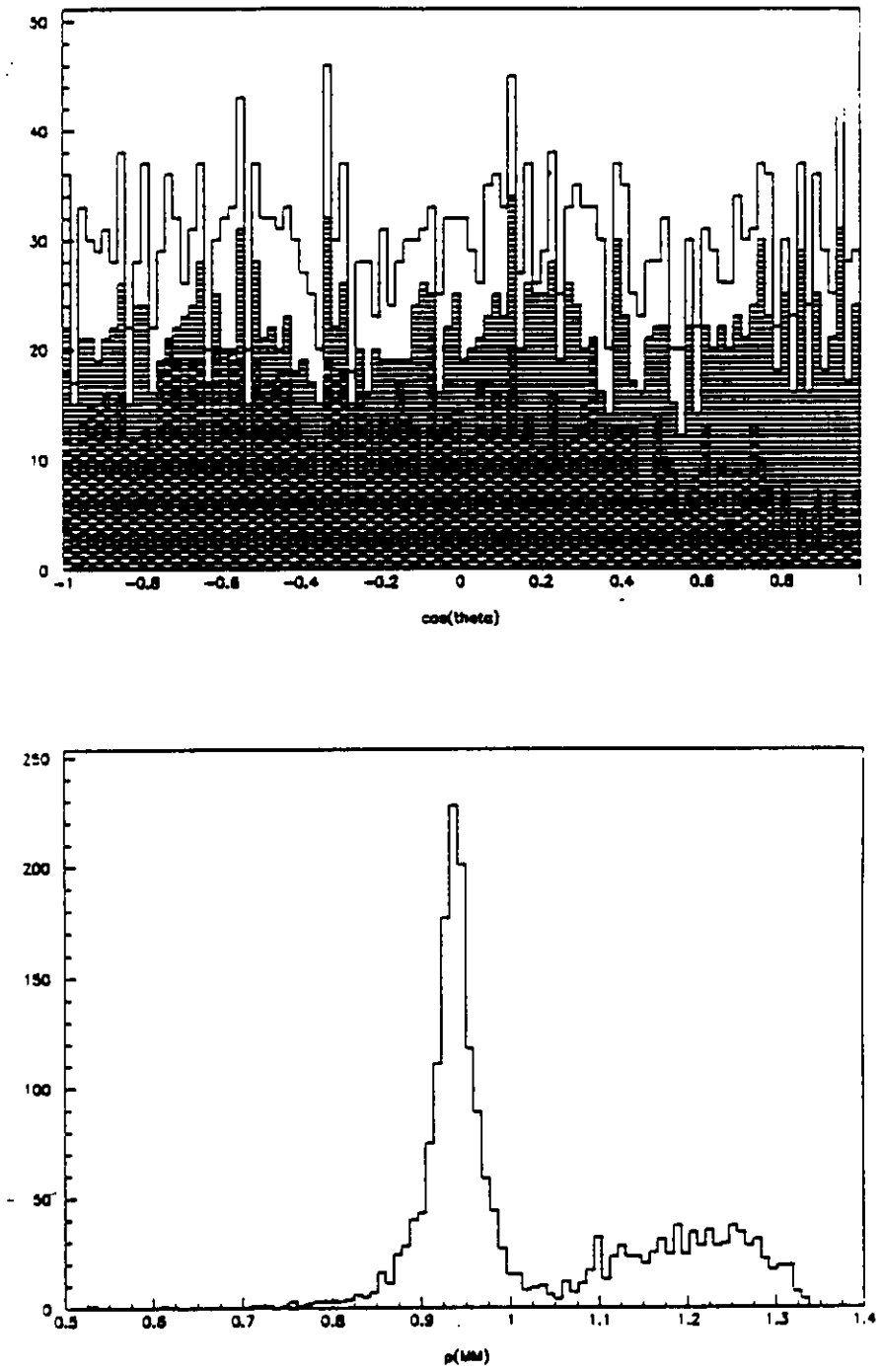

Figure 12. SDA simulation for phase space $\gamma d \rightarrow \pi^- p \pi^0 p_s$ at $E_\gamma = 0.7$ GeV: acceptance for π^- and p, respectively, versus the π^0 center of mass angle, cosθ (top). Missing mass peak of single pion channels mixed with two pion channels (bottom).

The following channels will contribute to the two pion production on the neutron:

$$\vec{\gamma} + \vec{d} \rightarrow \pi^- + p + \pi^0 + p_s \tag{3}$$

$$\vec{\gamma} + \vec{d} \rightarrow \pi^- + \pi^+ + n + p_s \tag{4}$$

$$\vec{\gamma} + \vec{d} \rightarrow \pi^0 + \pi^0 + n + p_s \tag{5}$$

The exclusive two-pion production study will mainly concentrate on the first two channels. The two outgoing charged particles will be detected, and the missing mass reconstruction technique will be used. Complete simulation has been done with a phase space angular distribution. It shows that CLAS will have complete angular coverage for multi-pion production channels. Fig.12 shows simulation results at a photon energy of 0.7 GeV. Multi-pion production has not yet been well studied. There have been some recent unpolarized two-pion production measurements up to 800 MeV from the DAPHNE group[34], but these are far from sufficient for a conclusive study. The polarization data from this experiment will certainly provide a new tool to study nucleon resonances. Our experiment will also be part of a large effort of the CLAS collaboration to study multi-pion production processes. Several approved experiments will study unpolarized two-pion and ω production.

3C. Inclusive single hadron production measurement

This is the primary measurement which will detect the contributions of all possible channels to the GDH sum rule in the region covered. We will 'count' whenever a hadron or photon triggers the detector. No missing mass reconstruction is needed since in this part of the experiment, we are measuring the total cross section. However, the measurements of the exclusive channels (3A and 3B) will greatly help the inclusive measurement for efficiency corrections and extrapolations.

The channels of the inclusive measurement which contribute to $\Delta\sigma$ are from single pion, multi-pion and other meson production.

The angular coverage is complete for multi-pion production, since one hadron will always get into the region covered by the detector. This is shown in our simulation mentioned in the previous section. As shown in section 3A, even for the single pion production channel, the angular coverage will be high. Single pion production is the best studied channel; partial-wave analysis fitted to the data from this experiment will provide an excellent means for extrapolating to the very forward and backward angles.

One concern that may arise is the detector efficiency for hadrons. When the hadron has very low momentum which is the case when the reaction is near two-pion or three-pion

threshold, the detector efficiency could be low. However, in the inclusive measurement, any track segment from region I pointing toward the target will be enough to identify the event. For channels with only neutral particles (for example: $\pi^0\pi^0 n$), since we only need to detect any one of the outgoing photons, the detection efficiency is not a problem. On the other hand, at the region very near the two-pion threshold, the cross sections for two-pion channels are much smaller than that of the single pion channels (see Fig.13). When the two-pion channel contributions become comparable to the single pion contributions, the momentum of one of the two pions will be reasonably high so that the detector efficiency will be good. The same argument holds for the case near the three-pion threshold.

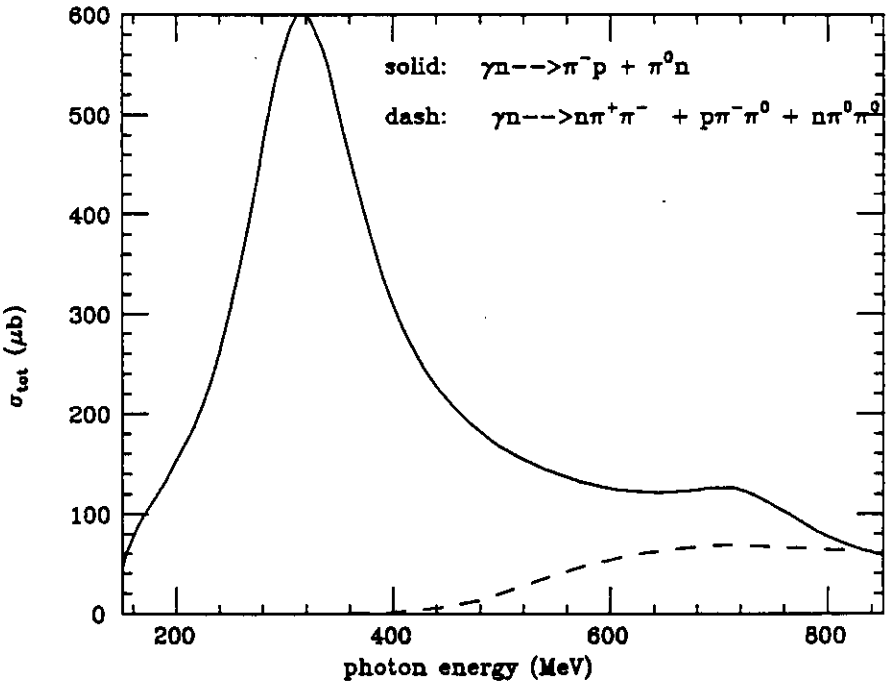

Figure 13. Total cross section of single pion photoproduction[4] compared with that of two pion photoproduction on the neutron[35]

4. Experimental Issues

In this section, we will address a few issues that are important for our proposed experiment.

4A. Trigger for neutral particle detection

In single $\pi^0 n$ production and in inclusive measurements, we need to detect outgoing neutral particles. Of particular concern are channels like $\gamma d \to \pi^0 + n + p_s$ or $\pi^0 +$

$\pi^0 + n + p_s$. For small π^0 angles ($< 90^0$), the decay photons can be detected in the calorimeter. When the π^0 angle is large, the outgoing neutron must be detected. In this kinematic region, where neutrons are emitted at small angle ($< 45^0$) and have relatively large momentum, the detection efficiency for the neutron is much higher (refer to Fig.6 and Fig.11). The requirement for neutron detection brings up a concern for the time window needed for the neutron trigger. Obviously, to minimize accidental rate, a small time window is desirable. With the above consideration in mind, and after a careful study, we plan to use a neutral particle trigger consisting of a threshold of about 100 MeV energy deposited in the calorimeters from one of the π^0 photons, or a threshold kinetic energy of 20 MeV and angle of less than 45^0 for the neutron either in a calorimeter or time-of-flight counter. The two triggers will cover those neutrons with low or high momenta respectively. The required time windows for this trigger are 35, 30 and 25 ns for incident electron energies of 0.8, 1.6 and 2.4 GeV respectively. The estimated accidental rates are shown in Table 4. The total rates are well below the CLAS limit in all cases. Off-line analysis guided by the timing information will eliminate these accidental backgrounds.

4B. Background and normalization

One of the major concerns when using other types of polarized targets (ND_3 or $C_4D_{10}O$) to test the GDH sum rule is the large background contribution from the heavy nuclei. However, with the new polarized HD ice target, this background is eliminated as the main concern.

Windows and other materials in the target will be about $(15 - 20)\%$ of the target material. Since all these material will not be polarized, they will not contribute to the cross section difference. Therefore, very clean measurements on the helicity cross section difference are expected. We plan to use the reactions $\gamma p \rightarrow \pi^+ n$ and $\gamma n \rightarrow \pi^- p$ in the Delta resonance region to calibrate our normalization factor. The unpolarized differential cross sections on these channels are quite well known in this region. The fact that there will be 5% aluminum by weight in the target and some window material makes it necessary to perform an empty target run with only the aluminum inside. This will allow us to subtract the background contributions.

4C. Nuclear corrections for bound deuteron

To extract the cross section difference $\Delta\sigma \equiv \sigma_{1/2} - \sigma_{3/2}$ for the neutron from the measured deuteron data, we need to subtract the contribution from the proton and to take into account the fact that the neutron is bound and has an internal momentum inside the deuteron. The first order correction can be made by taking into account the D-state of

the deuteron in a simple approach[36]:

$$\Delta\sigma_n = \frac{\Delta\sigma_d}{1 - 1.5 * \omega_d} - \Delta\sigma_p$$

where $\omega_d = 0.04$ is the probability of the deuteron to be in a D-state[37]. Realistic deuteron models can be used to further improve the extraction procedure. The extraction of the neutron data from the deuteron data is common to this proposal and the approved experiment E-93-009. The E-93-009 group has been working on this issue for some time now. We intend to work closely with them and with theorists to further understand the issue.

It is worthwhile to point out that, with the HD target, we will have measurements on both the free proton and the bound proton. The comparison of the single π^+ production on the deuteron with the single π^+ production on the proton will allow us to study the internal motion and the binding effects of the nucleon in deuteron.

V. Expected Experimental Results

Our goal in this experiment is to measure the helicity asymmetry for single and two pion production with high statistics and, adding the low energy measurements from BNL LEGS group, to test the GDH sum rule for the neutron to an accuracy of better than 10%, (or $\sim 20\mu b$) for the energy range from threshold ($\sim$ 150 MeV) to 2.2 GeV. For the test of GDH sum rule, the dominating uncertainty will be systematic. These systematic uncertainties will ultimately limit the accuracy we can achieve for testing the sum rule.

We will measure the cross section in energy bins of 25 MeV, consistent with the variations in the resonant structure of the cross section. For exclusive pion production, the differential cross section difference or asymmetry will be measured in angular bins of $\Delta\cos\theta = 0.1$ with a statistical uncertainty of $(2-9)\%$ depending on the channels and the kinematics.

5A. Systematic Uncertainty

Due to the $1/\nu$ weighting factor in the sum rule integral, the above uncertainty requirements are not as stringent as they may first appear to be. The systematic uncertainty in the total GDH sum (I) can be related to the uncertainty in each 25 MeV bin:

$$\delta I_{sys} = \delta_{sys}(\Delta\sigma) \ln \frac{\nu_{max}}{\nu_{min}}$$

where $\nu_{min} \approx 0.15$ GeV and $\nu_{max} \approx 2.2$ GeV. We would need $\delta_{sys}(\Delta\sigma) < 8\mu b$ to satisfy the requirement of $\delta I < 20\mu b$. Except in the Δ resonance peak, this requirement is never less than 10% of $\Delta\sigma$. Table 3 lists estimates for the major systematic uncertainties.

For the asymmetry measurements, some of the systematic uncertainties will largely cancel while others, which are helicity dependent, will not cancel. So the systematic uncertainty for the asymmetry measurements of the deuteron and the $\pi^- p$ channel will come mainly from beam and target polarization. For absolute cross section measurements, the normalization factor and detection efficiency will contribute to the systematic uncertainty as well. Since the neutron detection efficiency and the normalization factor are going to be calibrated simultaneously throughout the experiment, we can significantly reduce their uncertainties (refer to 2A and 4B).

Other uncertainty factors contributing to the GDH sum rule measurements on the neutron are the subtraction of the proton contributions, the nuclear correction for bound neutrons and the extrapolation into unmeasured angular regions. For our exclusive production measurements, the asymmetry is for each energy and angular bin, and no extrapolation is needed. The estimated uncertainty, 3%, for the extrapolations in the sum rule measurements is very conservative (refer to 3C).

Table 3. Systematic Uncertainties

Sources	Uncertainty
(A) Factors affecting cross section but not asymmetry	
Normalization factor (photon flux, target thickness)	3%
Detection acceptance and efficiency	4%
(B) Factors directly affecting asymmetry	
Polarization (beam and target)	5%
Total for Deuteron	7%
Proton subtraction & binding effects	5%
Extrapolation	3%
Total for Neutron (Sum Rule)	9%

5B. Statistical uncertainty

For single pion asymmetry measurements, a statistical accuracy of $\leq 5\%$ for $\nu = 0.28 - 2$ GeV is desired. For the sum rule test, the statistical uncertainty should be smaller than the systematic uncertainty. Since the statistical uncertainties in each energy bin are

uncorrelated, a constant statistical uncertainty $\delta_{stat}(\Delta\sigma)$ in each energy bin of width $\Delta\nu$ will give a statistical uncertainty in the sum rule

$$\delta I_{stat} = \delta_{stat}(\Delta\sigma)[\Delta\nu(\frac{1}{\nu_{min}} - \frac{1}{\nu_{max}})]^{1/2}$$

With a $\delta_{stat}(\Delta\sigma) < 5\mu$b for each 25 MeV bin, the statistical uncertainty in the sum rule is $\delta_{stat} I < 2\mu$b, which is much smaller than the estimated systematic uncertainty.

The statistical uncertainties in the difference of cross sections are

$$\delta_{stat}(\Delta\sigma) \approx \frac{2\sigma}{Pf\sqrt{Tc}}$$

where σ is the unpolarized cross section, P is the product of photon and target polarizations, f is the target dilution factor ($f = 2/3$ for deuteron and 1/3 for proton for a HD target), T is the counting time and C is the counting rate

$$C = N_\gamma \times N_t \times \sigma \times \epsilon\Omega$$

where N_γ is the tagging photon rate, N_t is the number of target nuclei, and $\epsilon\Omega$ is the solid angle acceptance (including efficiency factor) for the detector.

The statistical uncertainties in the asymmetry $E(\theta)$ are

$$\delta_{stat}(E(\theta)) \approx \frac{1}{Pf\sqrt{Tc(\theta)}}$$

where $C(\theta)$ is the counting rate for a θ bin.

5C. Count rates and run times

To estimate the counting rates, we assume the following:

N_γ:	10^7 tagged γ/sec in the specified photon energy range
target thickness:	7 cm HD or 1.1 g/cm^2
target diameter:	2.5 cm, photon beam collimated to 2 cm
geometrical efficiency:	50% $\times 4\pi$
electron polarization:	80%
target polarization:	50% for deuteron, 80% for proton
energy bin width:	25 MeV
angle bin width:	$\Delta \cos\theta = 0.1$.

The estimated counting rates are listed in Table 4, and the run times (including empty target runs) are listed in Table 5. Expected 'data points' with estimated total uncertainties (statistical and systematic) in $E(\theta)$ from extensive SDA simulation are plotted in Figure 14.

Expected total error for the GDH sum rule, together with the VPI GDH integral calculation and several model calculations, are plotted in Figure 15. If we assume that the total uncertainty for the proton measurement is $12\mu b$, then the total error of the GDH sum rule for the proton-neutron difference will be $23\mu b$. We should be able to distinguish clearly between the prediction from the GDH sum rule and from ref.14.

Table 4. Real Counting Rates and Accidental Rates

E_0 (GeV)	ν_{min} (GeV)	ν_{max} (GeV)	Tagged γ on target (10^7/s)	$\gamma \geq 0.15GeV$ on target (10^7/s)	window (ns)	Tagged real rate (1/s)	Accidental rate (1/s)
0.8	0.28	0.76	0.270	0.437	35	280	15
1.6	0.70	1.52	0.569	1.700	30	310	200
2.4	1.40	2.28	0.733	4.13	25	420	470

Table 5. Beam Time Request (Hours)

E_0(GeV)	ν_{min}(GeV)	ν_{max}(GeV)	Run Time
0.8	0.28	0.76	85+15
1.6	0.72	1.52	100+20
2.4	1.44	2.28	120+20

VI. Summary

With the advances in polarized electron and photon beams, and in polarized targets, it has now become possible to perform double polarization measurements. Making full use of the polarized tagged photon facility and the CLAS detector, and introducing a novel polarized solid HD target, we will be able to measure the asymmetry in single pion production on the neutron, which has never been measured before, to about $(2-6)\%$ and helicity cross section difference for exclusive two-pion production to 4-9%. Also we will measure the GDH sum from 0.28 to 2.2 GeV, covering most of the resonance region. Combining our data with low energy measurements from BNL, we will be able to test the

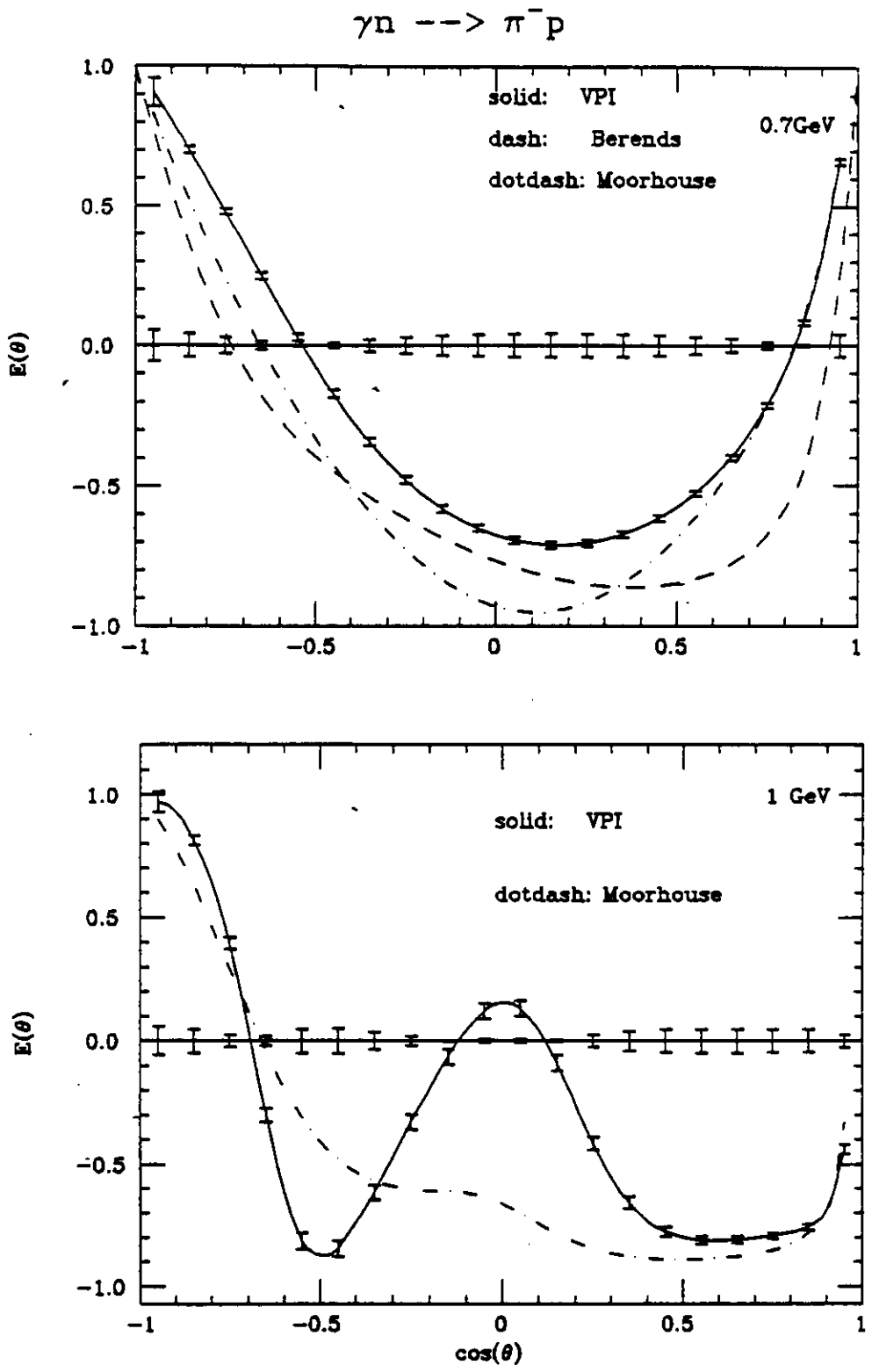

Figure 14. Helicity asymmetry for $\gamma n \rightarrow \pi^- p$ calculated from the three different partial-wave analyses[4],[5],[6]*. 'Data' points are results expected from this experiment. Expected systematic errors are plotted on the x-axis.*

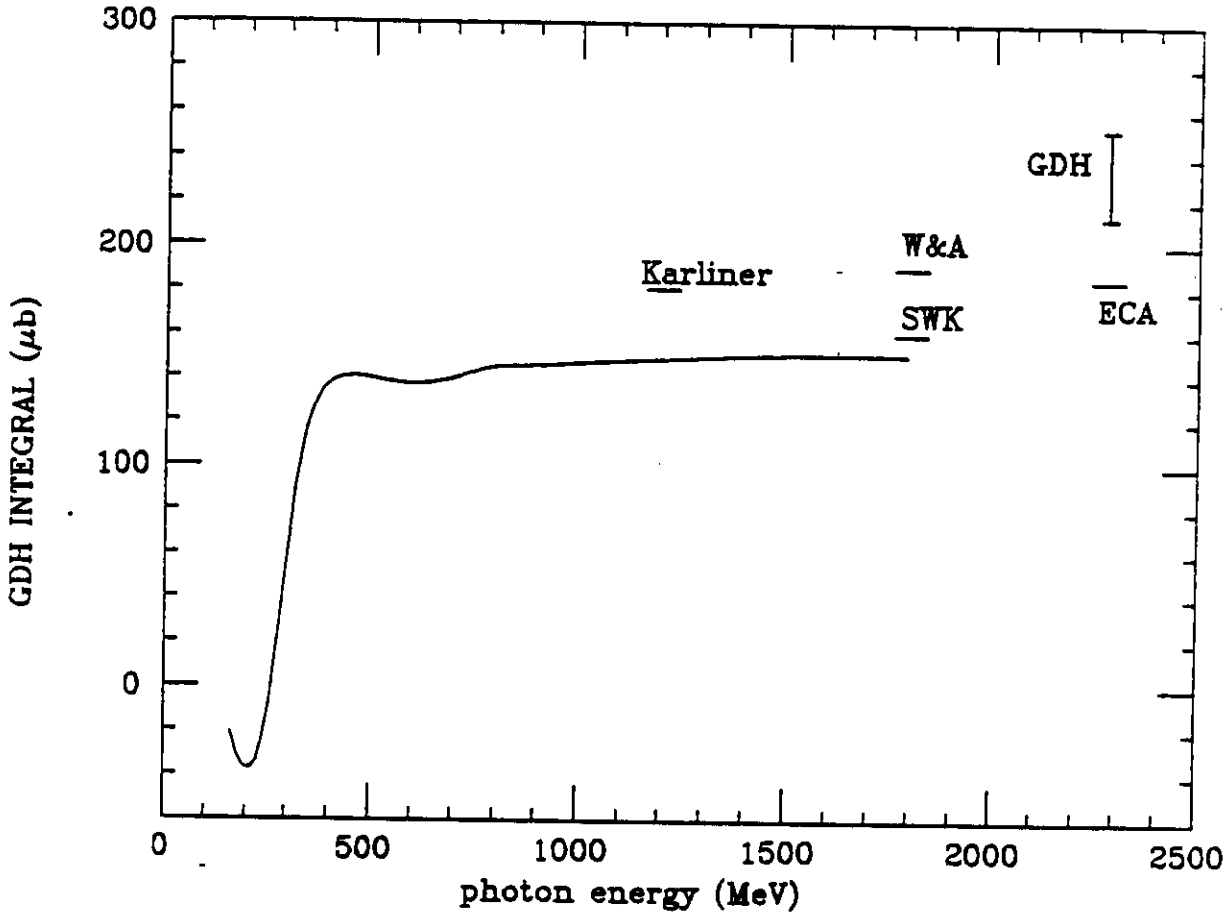

Figure 15. Expected GDH sum rule data points compared with several model calculations (Karliner[10], W&A[11], SWK[13] and ECA[14]; the solid curve is the GDH integral calculated using VPI single pion production partial-wave amplitudes.)

GDH sum rule to about $20\mu b$. All measurements can be done consecutively with identical conditions to the proton measurements. The proton proposal has already been approved for 18 days (assumed 50% electron polarization) for the energy range from 0.28 to 2.2 GeV.

A feasibility study on extending the measurements to a photon lab energy of 3.8 GeV will be considered. It would test the convergence of the GDH rum rule beyond the resonance region.

References

[1] W. Meyer, Frontiers of High Energy Spin Physics, p165 (1992).

[2] G. Blanpied et al., PRL 69, 1880(1992); Few-Body systems, Suppl. 7, 317.

[3] R. Kajikawa, Proc. on Lepton and Photon Interactions at High Energies, 352 (1981).

[4] Zh. Li, R. Arndt, L. Roper, R. Workman, Phys. Rev. C47, 2759 (1993).

[5] F. A. Berends and A. Donnachie, Nucl. Phys. B84, 342 (1975); B136, 317 (1978).

[6] R.G. Moorhouse, Phys. Rev. D Vol.9, 1(1974).

[7] S. Capstick, Phys. Rev. D46, 2864(1992).
R. Koniuk and N. Isgur, Phys. Rev. D21, 1868(1980).

[8] S. B. Gerasimov, Sov. J. Nucl. Phys. 2, 430 (1966).
S. D. Drell and A. C. Hearn, Phys. Rev. Lett. 16, 908 (1966).

[9] F. E. Low, Phys. Rev. 96, 1428 (1954).
M. Gell-Mann and M. L. Goldberger, Phys. Rev. 96, 1433 (1989).

[10] I. Karliner, Phys. Rev. D7, 2717(1973).

[11] R.L. Workman and R.A. Arndt, Phys. Rev. D45, 1789(1992).

[12] V. Burkert and Zh. Li, Phys. Rev D47. 46(1993).

[13] A.M. Sandorfi, C.S. Whisnant and M. Khandaker, Phys. Rev. D50, 11(1994).

[14] L. N. Chang, Y. Liang and R. L. Workman, Phys. Lett. B329, 514 (1994).

[15] M. Anselmino, B. L. Ioffe and E. Leader, Sov. J. Nucl. Phys.
V. Burkert and B.L. Ioffe, Phys. Lett. B296, 223(1992).
V. Burkert and B.L. Ioffe, JETP 105, 1153(1994). 49, 136 (1989).

[16] J. Ashman *et al.*, Nucl. phys. B328, 1 (1989) .

[17] G. Baum *et al.*, Phys. Rev. Lett. 45, 2000 (1980) and 51, 1135 (1983).

[18] K. Abe *et al.*, SLAC-PUB-6508, submitted to PRL..

[19] B. Adeva *et al.*, Phys. Lett. B302, 533 (1993).

[20] P. L. Anthony *et al.*, Phys. Rev. Lett. 71, 959 (1993).

[21] J. D. Bjorken, Phys. Rev. 179, 1547 (1969).

[22] CEBAF-E-91-023, V. Burkert, D. Crabb and R. Minehart *et al.* (1991).
CEBAF-E-93-009, S. E. Kuhn *et al.* (1993).
CEBAF-E-94-015, Z.Meziani *et. al.* (1994).

[23] CEBAF-E-91-015, D. I. Sober *et al.* (1991).

[24] *Sum rule measurements of the spin-dependent Compton amplitude*, LEGS-Spin-Collaboration, BNL-61005 (1994).

[25] H.Olsen and L.C. Maximon, Phys. Rev. 114, 887(1959).

[26] A. Honig, Q. Fan, X. Wei, A. M. Sandorfi and C. S. Whisnant, 7th Workshop on Polarized Target Materials and Techniques, Bad Honnef, Germany, June 20-22, 1994. To be published in Nucl. Instrum. and Meth..

[27] N. Alexander, J. Barden, Q. Fan and A. Honig, Rev. Sci. Instr. 62, 2729 (1991).

[28] R. M. Kulsrud, H. P. Furth, E. J. Valeo and M. Goldhaber, Phys. Rev. Lett. 49, 1248 (1982).

[29] Y.-L. Pan and S. P. Hatchett, Nucl. Fusion 27, 815 (1987).

[30] A. Honig and H. Mano, Phys. Rev. B14, 1858(1976).

[31] CEBAF *Conceptual Design Report*, 1990.

[32] W. Brooks, CEBAF-E-94-017.

[33] T. Amstrong, *et al.*, Nucl. Phys. B41, 445 (1972)

[34] A.Braghieri and L. Murphy et. al., submitted to Phys. Lett. B, 1994.

[35] L. Murphy and J.-M. Laget, private communication.

[36] M. Lacombe *et al.*, Phys. Lett. B101, 139 (1981).

[37] B. Desplanques, Phys. Lett. B203, 200 (1988).

Appendix: Principle of Operation of The SPHICE Target

A. Relaxation Switch

The symmetry restrictions imposed on the total wave functions of H_2 (two fermions) and D_2 (two bosons) limit the possible nuclear spin orientations at low temperature. For hydrogen at room temperature, the most abundant species, the so-called ortho state, is nuclear spin, I=1 and molecular orbital angular momentum, J=odd. The equilibrium condition at low temperature is the para-hydrogen state with I=0 and J=0. In the case of deuterium, it is the p-D_2 combination (I=1; J=odd) that disappears at low temperature, leaving the o-D_2 (I=0,2; J=0). In contrast, the orbital and spin angular momenta of the heteronuclear molecule HD is not limited by symmetry requirements and hence can be in the molecular-rotation state J=0 independent of the H or D spin orientations at low temperature. Since the spin-lattice coupling is primarily by way of the molecular rotations, the relaxation rates are exceedingly small, corresponding to relaxation times of days even at 4 K. Although this long relaxation time is essential for usable targets, it makes the polarization phase equally long. The solution to this problem was suggested by Honig[1] in 1967. The relaxation (polarization) time can be reduced by introducing small ($\approx 10^{-4}$) concentrations of o-H_2 and p-D_2.

The presence of o-H_2 and p-D_2 are important for the polarization process since the molecular orbital angular momentum couples with both the lattice and the nuclear spin. The transitions from o-H_2 to p-H_2 and from p-D_2 to o-D_2 occur with time constants of 6.25 and 18.25 days, respectively. These rates are independent of temperature and applied magnetic field. Thus, for H_2 and D_2 the spin-lattice coupling that makes polarization (and depolarization) possible is time dependent.

Although the o-H_2 and p-D_2 decay rates are independent of temperature and applied magnetic field, the polarization relaxation times for hydrogen and deuterium in HD are a function of the o-H_2 and p-D_2 concentrations and the temperature and magnetic field. The hydrogen and deuterium relaxation times are long for small o-H_2 and p-D_2 concentrations and large magnetic fields[2]. Thus, by doping the pure HD with o-H_2 and p-D_2 the relaxation times of the H and D in HD are reduced so that the sample may be polarized.

To produce a practical target, the relaxation times must be increased after the target is polarized so that it is in a metastable state and can be removed from the high field/low temperature conditions for use as a target. The choice of o-H_2 and p-D_2 as the magnetically active impurities provides a natural mechanism for achieving this since they decay to the magnetically inert p-H_2 and o-D_2. This provides the so-called "relaxation switch": by simply holding the target at the low temperature and high field conditions, the relaxation

times will increase as the impurity concentrations decline.

B. Initial Polarization

A suitably doped HD sample is polarized at high magnetic field and low temperature. The proton and deuteron spins relax, aligning with the magnetic field and transferring the transition energy to the lattice. On a time scale set by the initial doping concentrations, the equilibrium polarization may be achieved. The equilibrium (vector) polarization for nuclei of spin I are given as a function of the ratio of the magnetic field, B, and the temperature, T, by the Brillouin function

$$P_I(B/T) = \frac{2I+1}{2I} coth\left(\frac{(2I+1)g\mu_N B}{2kT}\right) - \frac{1}{2I} coth\left(\frac{g\mu_N B}{2kT}\right). \quad (1)$$

where g is the nuclear g-factor, k is the Boltzman constant and μ_N is the nuclear magneton. Since the population of the magnetic sub-states is characterized by a temperature which determines the Boltzman factor, $e^{-E/kT}$, the vector and tensor polarization (or alignment) of the deuteron are not independent[3], but are related by

$$A = 2 - \sqrt{4 - 3P_I^2}. \quad (2)$$

The production of high polarizations by relaxation requires the use of a dilution refrigerator and a superconducting magnet. For the production of the SPHICE target, we will cool the target to 15-20 mK and use a magnetic field of 17 Tesla. The equilibrium polarizations that can be achieved are shown in Figure 1. The equilibrium values achieved for 17 Tesla and 15 mK are indicated on the figure.

Although the dilution refrigerator is capable of reaching 10 mK, due to the heat generated internally from the decay of the J=1 H_2 and D_2 species, the base temperature of the target is about 15 mK. This limitation is described below in the section discussing the feasibility study results.

C. Deuterium Polarization

Increasing the deuterium polarization to a more desirable level requires that another technique be employed. Honig and Mano[4] demonstrated that a variation of the so-called "solid effect" can be used to transfer the polarization of the hydrogen to the deuterium. This technique takes advantage of the dipolar coupling of H and D nuclei in different HD molecules. The energy level diagram for the coupling of a single H and a single D on neighboring HD molecules is shown in Figure 2.

Although the states, labeled **a-f**, can be approximately characterized by the high field quantum numbers, m_H and m_D, the dipolar coupling introduces admixtures of other

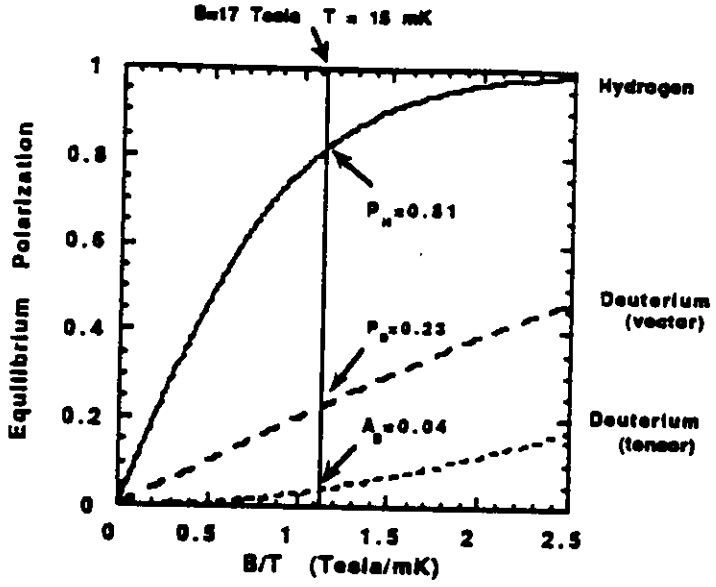

Figure 1. Equilibrium polarizations for hydrogen and deuterium as a function of the ratio B/T. The 14 Tesla, 15mK conditions indicated correspond to that planned for the SPHICE target.

states. This dipole coupling causes a fraction of the states with (m_H, m_{D+1}) to be added to the states (m_H, m_D). By inducing these 'forbidden' transitions, the polarization of the proton can be transferred to the deuteron. At a fixed value of the external magnetic field, B_0, the transitions $\mathbf{b} \leftrightarrow \mathbf{d}$ and $\mathbf{c} \leftrightarrow \mathbf{e}$ occur at a lower frequency than the $\mathbf{a} \leftrightarrow \mathbf{e}$ and $\mathbf{b} \leftrightarrow \mathbf{f}$ transitions. Thus, by proper choice of the rf field frequency, one can select the direction to induce these transitions. By sweeping through the resonant frequency, the populations of the affected states can be inverted. Using this adiabatic fast passage technique, polarization is transferred from the hydrogen to the deuterium.

Since the transition rate is proportional to the strength of the rf field, B_1, this can be chosen so that the forbidden transitions can be saturated in less than 1 minute. Reducing B_0 to about 0.03T increases the field uniformity and shifts the NMR frequencies to convenient range. Since the spin-lattice relaxation time is already > 0.5 hr even at this modest field, there is no significant loss in polarization. The adiabatic fast passage technique is now employed to invert the populations of the appropriate magnetic substates. The maximum possible polarization transfer is 2/3 of the hydrogen polarization. Practical limitations presently reduce this to 1/3. This, however, does not limit the deuterium polarization to 1/3 of that for hydrogen. Depending on the choice of initial impurity concentrations and the history of the sample, several options are available. Starting from $\approx 10^{-4}$ concentrations of both o-H_2 and p-D_2, both the hydrogen and deuterium will be polarized during

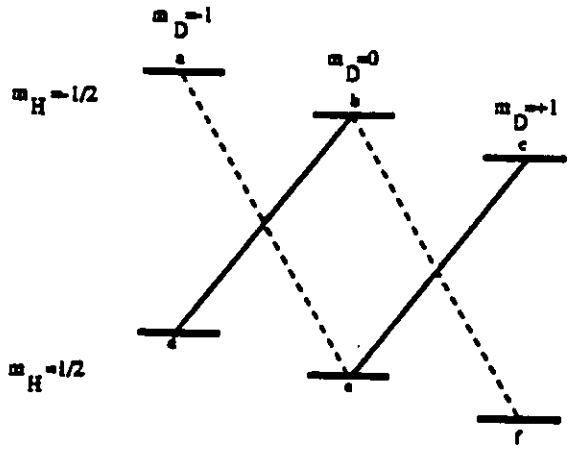

Figure 2. Magnetic energy levels of dipolar coupled H and D nuclei on neighboring HD molecules. "Forbidden" transitions are shown by lines connecting states.

the initial relaxation.

Because of the longer decay time for the p-D_2, the target production time is shortened by doping only with o-H_2. The feasibility study demonstrates that even if the initial p-D_2 is very small, initial deuterium polarizations of 4-5% are achieved. This arises due to a weak coupling of the deuterium to the lattice through the o-H_2 impurities. The polarization transferred from the hydrogen is then added to this initial value, not to zero. As the o-H_2 concentration decreases, this small coupling becomes irrelevant and the deuterium polarization is retained.

Deuterium polarization can also be increased by repeating the transfer, repolarizing the hydrogen at high field after each iteration. Because the relaxation time is constantly increasing, there is a window of opportunity for these transfers. If the relaxation time is too short, significant polarization is lost during the low field rf transitions and if too long the hydrogen cannot be repolarized. This places a practical limit at two transfers during the target production cycle. Taking into account the changing o-H_2 concentration and target temperature, using the achieved transfer efficiency of 50% and assuming no initial deuterium polarization, the time line for a target production cycle is shown in Figure 3.

Once polarized, the target must be held at high field and low temperature until the o-H2 and p-D2 have decayed and the relaxation time increases. In this way it is possible to make HD ice targets with at least a 50% deuteron vector polarization and a tensor polarization of 20%.

D. Feasibility Study Results

For the present experiments in which polarized D and/or polarized H are desirable, a presumption could be made that additional aging time would increase the relaxation

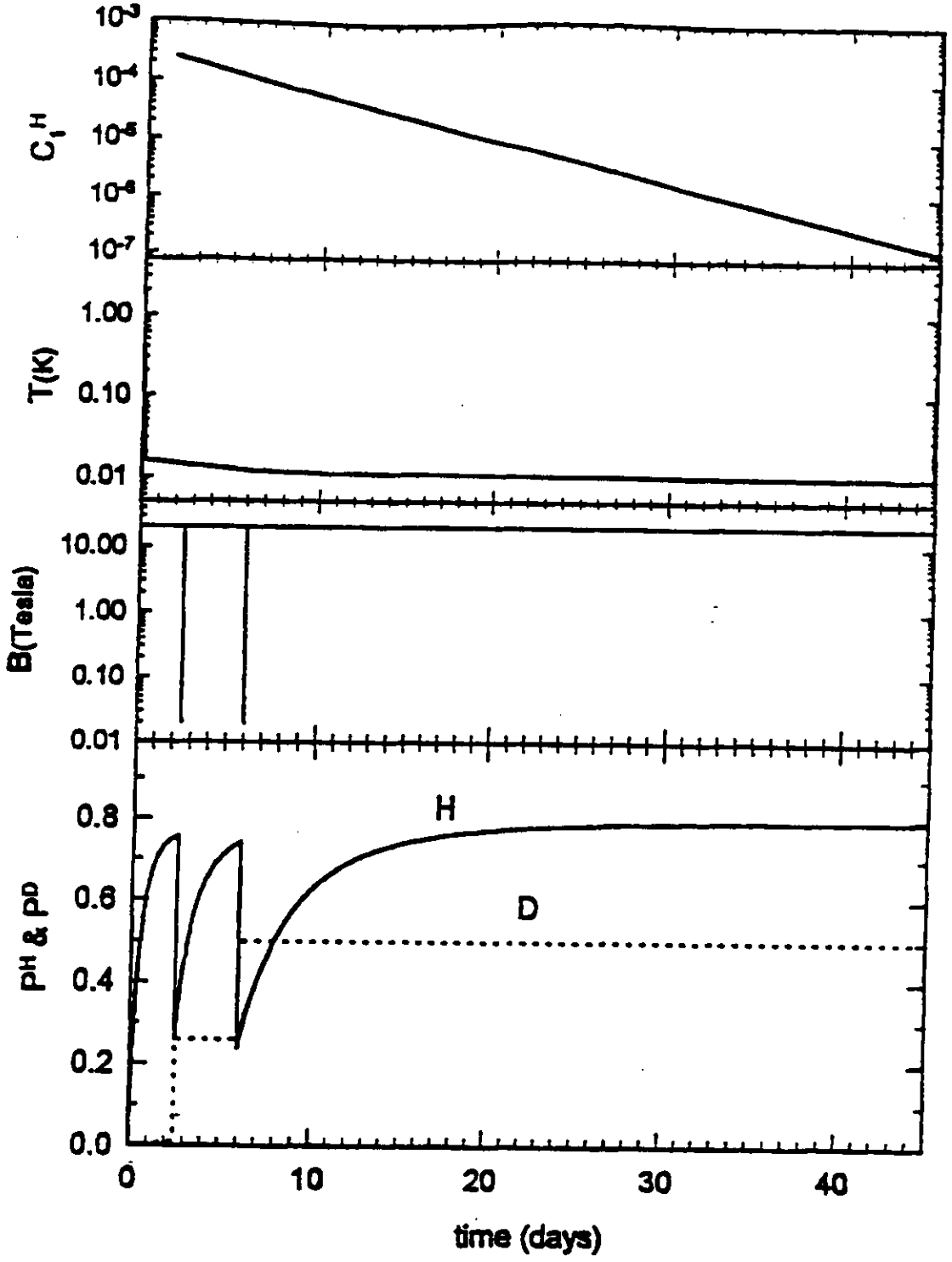

Figure 3. The time-line for polarizing the SPHICE target. C_1^H (upper panel) is the concentration of J=1 ortho-H_2. The H-polarization continuously increases as the o-H_2 concentration decreases. At day 2.5 and day 6 polarization transfer from H → D is induced by "forbidden" Rf-transitions. The resulting H and D polarizations are shown as the solid and dotted curves in the lower panel.

times of H as well as of D to the point where the polarization retention and production times match. This presumption is by no means self-evident, since relaxation times in the range of weeks to months had never been explored before the feasibility study conducted by the LEGS-Spin collaboration. One eventually expects a weak relaxation mechanism intrinsic to the HD to begin controlling the relaxation, after which further reductions of c_1^H and c_1^D by aging would have no effect. Tests of the limits of T_1^H and T_1^D after aging periods of months was one focus of our feasibility study. The successful outcome has been reported[5],[6], and is summarized here.

The results of the target aging tests conducted at 1.5K, the operating temperature of the in-beam dewar, are shown in Figure 4. Most of the experiments used HD samples in long glass tubes with a reservoir for containing the HD in the gas phase. This storage vessel makes the samples easy to transfer in and out of a variable temperature dewar. These "open geometry" results are indicated with the filled symbols. As seen from the figure, the relaxation times for deuterium are always longer than for hydrogen.

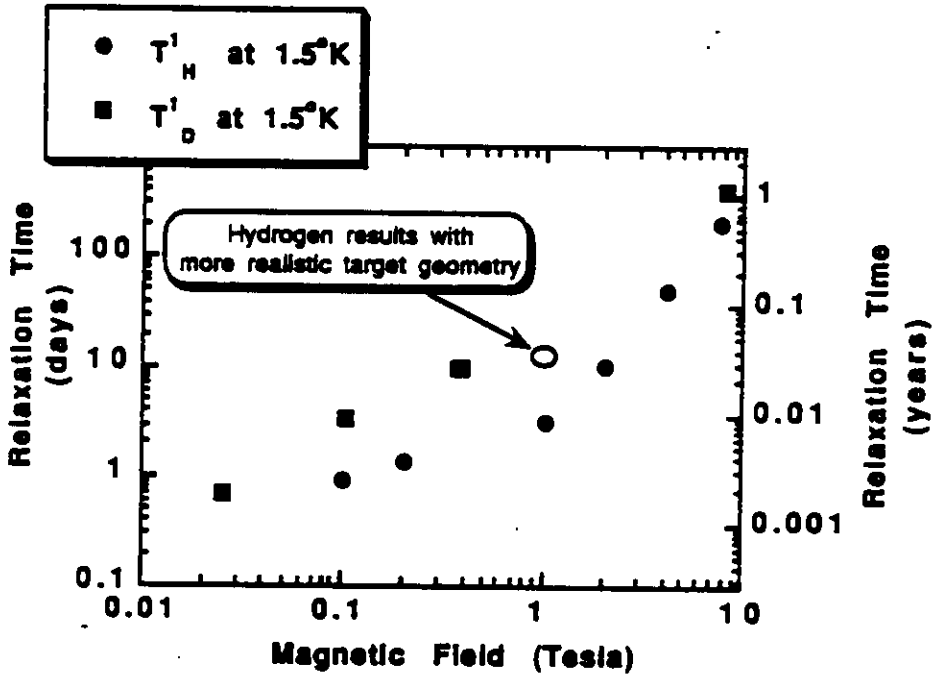

Figure 4. The polarization relaxation time as a function of magnetic holding field at 1.5K.

At a holding field of 2T, hydrogen relaxation times of about 10 days are sufficient for a practical target. Subsequent measurements were done in a dilution refrigerator with a closed target geometry more closely approximating that to be used for the production target. The result at 1T is shown as the open circle indicating that a 13 day relaxation time for hydrogen can be achieved at this lower field. Lowering the holding field reduces the cost of the in-beam magnet and is more convenient for use in CLAS.

Additional measurements have been made at 0.45K and the hydrogen relaxation times are at least a factor of two longer than at 1.5K. Thus, by pumping on ^{3}He rather than ^{4}He, a substantial increase in the relaxation time is realized. For constant time in-beam, this means a higher average target polarization. For example, if a target is used for one mean lifetime in the beam, the average polarization is 63% of the initial value. If, however, the mean life is four times the usage time the average polarization is 88% of the initial value, a substantial increase. Producing 4 targets each with a lifetime of a month and using them for a week results in an average polarization of 88% of the initial value. Since the relaxation times for deuterium are longer than for the hydrogen, the polarization losses are even smaller and the resulting average polarizations are comparable to existing targets.

These experiments also set the scale for the aging time required to produce a target with a usable lifetime. The results shown in Figure 4 correspond to aging times of about 45 days. To make these long times practical, a plan for producing four targets in one production cycle has been devised. Thus, in one production cycle, four targets each with greater than one week useful lifetime at 1T and 1.5K will be produced. The very long relaxation times at high field, near one year at 7T, make storage for later usage practical[5],[6].

The second main issue addressed in the feasibility study was the heat removal in the large volume targets. At the low temperatures encountered during the polarization phase, HD has a very poor thermal conductivity. Typical initial c_1^H values of 3×10^{-4} generate in HD a conversion heat of about 0.8 μW/mole. To prevent large thermal gradients, this heat is removed by threading thin wires through the target. The minimum wire density is determined by the thermal boundary resistance, or Kapitza resistance, between the wires and the HD in the target. By threading 25 μm copper or gold plated aluminum wires through the target with a density of 6 wires/mm^2, an acceptable solution is obtained. Using a 0.49 cm diameter by 1.3 cm long sample doped with concentrations of J=1 H_2 and D_2 to give a target heating rate comparable to that encountered at the beginning of the polarization cycle, the sample could be reduced to 20 mK. As the concentrations decrease, so does the heat load and the temperature was reduced to about 15 mK after about 10 days of aging. Also, this density of wires is sufficient to keep the thermal gradients in the target to below 2 mK for targets up to 10 cm in length (and any area). Since aluminum and copper both perform well, aluminum was chosen to reduce the number of extraneous nuclei in the target. With this density of wires, the target is 5% aluminum by weight. This means that the number of nucleons in Al nuclei is 14% of the number of hydrogen or deuterium nuclei.

References

[1] A. Honig, Phys. Rev. Lett. 19, 1009 (1967).

[2] A. Honig, "Evaporation of Solid Polarized HD and Pure Ortho-D_2", Eighth International Symposium on High Energy Spin Physics, Vol. 2, Minneapolis, MN, 1998. AIP Conference procedings 189, 1554(1989).

[3] W. F. Kielhorn, Ph.D. thesis, University of Texas, Austin. Los Alamos report LA-12116-T, (unpublished).

[4] A. Honig and H. Mano, Phys. Rev. B14, 1858 (1976).

[5] A. Honig, Q. Fan, X. Wei, A. M. Sandorfi and C. S. Whisnant, 7th Workshop on Polarized Target Materials and Techniques, Bad Honnef, Germany, June 20-22, 1994. To be published in Nucl. Instrum. and Meth.

[6] A. Honig, Q. Fan, X. Wei, M. Rigney, A. M. Sandorfi and C. S. Whisnant, Paper presented at the Eleventh Intl. Symp. on High Energy Spin Physics and the Eighth Intl. Symp. on Polarization Phenomena in Nuclear Physics, Bloomington, Indiana, Sept. 15-22 (1994).

BEAM REQUIREMENTS LIST

CEBAF Proposal No.: _____ Date: _____
(For CEBAF User Liaison Office use only.)

List all combinations of anticipated targets and beam conditions required to execute the experiment. (This list will form the primary basis for the Radiation Safety Assesment Document (RSAD) calculations that must be performed for each experiment.)

Condition #	Beam Energy (MeV)	Beam Current (μA)	Polarization and Other Special Requirements (e.g., time structure)	Target Material (use multiple rows for complex targets — e.g., w/windows)	Target Material Thickness (mg/cm^2)
	800	<0.01	80%	ice HD	1100 mg/cm^2
	1600	<0.01	80%	Mylar	71 mg/cm^2
	2400	<0.01	80%	Aluminum	51 mg/cm^2
			Tagging photon: 10^7/s		

The beam energies, E_{Beam}, available are: $E_{Beam} = N \times E_{Linac}$ where N = 1, 2, 3, 4, or 5. For 1995, E_{Linac} = 800 MeV, i.e., available E_{Beam} a. 800, 1600, 2400, 3200, and 4000 MeV. Starting in 1996, in an evolutionary way (and not necessarily in the order given) the following additional values of E_{Linac} will become available: E_{Linac} = 400, 500, 600, 700, 900, 1000, 1100, and 1200 MeV. The sequence and timing of the available resultant energies, E_{Beam}, will be determined by physics priorities and technical capabilities.

HAZARD IDENTIFICATION CHECKLIST

CEBAF Proposal No.: _____ Date: _____
(For CEBAF User Liaison Office use only.)

Check all items for which there is an anticipated need.

Cryogenics
- ____ beamline magnets
- ____ analysis magnets
- x target
  - type: Liquid He
  - flow rate: _____
  - capacity: _____

Electrical Equipment
- ____ cryo/electrical devices
- ____ capacitor banks
- ____ high voltage
- ____ exposed equipment

Radioactive/Hazardous Materials
List any radioactive or hazadorous/toxic materials planned for use:
_____
_____
_____
_____

Pressure Vessels
- ____ inside diameter
- ____ operating pressure
- ____ window material
- ____ window thickness

Flammable Gas or Liquids
- type: _____
- flow rate: _____
- capacity: _____

Drift Chambers
- type: _____
- flow rate: _____
- capacity: _____

Other Target Materials
- ___ Beryllium (Be)
- ___ Lithium (Li)
- ___ Mercury (Hg)
- ___ Lead (Pb)
- ___ Tungsten (W)
- x Uranium (U)
- ___ Other (list below)
  pol. ice HD target
  _____

Vacuum Vessels
- ____ inside diameter
- ____ operating pressure
- ____ window material
- ____ window thickness

Radioactive Sources
- ____ permanent installation
- ____ temporary use
- type: _____
- strength: _____

Large Mech. Structure/System
- ____ lifting devices
- ____ motion controllers
- ____ scaffolding or
- ____ elevated platforms

Lasers
- type: _____
- wattage: _____
- class: _____

Installation:
- ____ permanent
- ____ temporary

Use:
- ____ calibration
- ____ alignment

Hazardous Materials
- ___ cyanide plating materials
- ___ scintillation oil (from)
- ___ PCBs
- ___ methane
- ___ TMAE
- ___ TEA
- ___ photographic developers
- x other (list below)
  solid HD ice
  _____

General:

Experiment Class:

- ____ Base Equipment
- x Temp. Mod. to Base Equip.
- ____ Permanent Mod. to Base Equipment
- ____ Major New Apparatus

Other: _____
_____

LAB RESOURCES REQUIREMENTS LIST

CEBAF Proposal No.: _____ Date: _____
(For CEBAF User Liaison Office use only.)

List below significant resources — both equipment and human — that you are requesting *from CEBAF* in support of mounting and executing the proposed experiment. Do not include items that will be routinely supplied to all running experiments, such as the base equipment for the hall and technical support for routine operation, installation, and maintenance.

***Major Installations** (either your equip. or new equip. requested from CEBAF)*

New polarized ice HD target including a 1 Tesla holding magnet. 1° K refrigerator and polarized target material. All provide by user, but needs CEBAF support for installation

New Support Structures: _____

Data Acquisition/Reduction

Computing Resources: _____

New Software: _____

Major Equipment

Magnets: standard

Power Supplies: standard

Targets: polarized ice HD

Detectors: standard

Electronics: standard

Computer Hardware: standard

Other: _____

Other